2024 IEEE Photonics Conference (IPC)
Rome, Italy, 10 - 14 Nov 2024

FA9550-20-1-0135 AFOSR
FA9550-24-1-0061 AFOSR
DMR-2235447 NSF
DMR-2423992 NSF

Accurate measurements and models of temperature-dependent optical constants for infrared detector materials

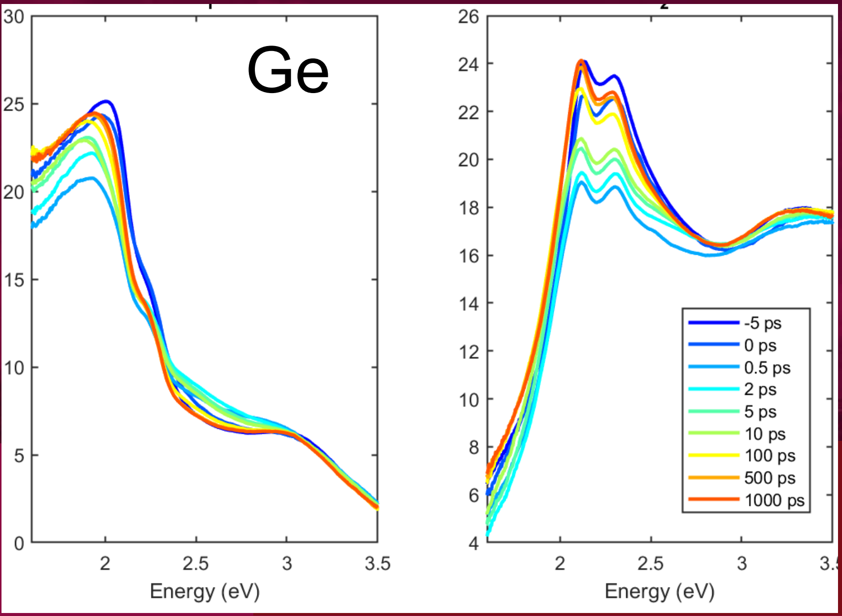

Stefan Zollner

With Carlos A. Armenta, Carola Emminger, Sonam Yadav, Melissa Rivero Arias, Jaden R. Love (NMSU), Jose Mendendez (Arizona State)

Department of Physics, New Mexico State University, Las Cruces, NM, USA
Email: zollner@nmsu.edu. WWW: http://femto.nmsu.edu.

Precision measurements of optical constants

1) <u>Bulk materials</u>: Semiconductors, metals, insulators
   SiC, $SrTiO_3$, AlSb, Ge, GaAs, GaP, GaSb, InSb, SiC (4H and 6H), Ni, Pt, Au, $MgAl_2O_4$, NiO (excitons), LiF, LSAT, $ZnGa_2O_4$, $LaAlO_3$
2) <u>Epitaxial layers</u> (CVD, MBE, ALD):
   NbO_2, Co_3O_4, $SrTiO_3$ (doped, quantum wells), $BaSnO_3$, ZnO, SnO_2,HfO_2, $Gd_xGa_{2-x}O_3$, silicides, SiGe:C, GeSn, $GaAs_{1-x}P_x$, alpha-tin on InSb and CdTe, native oxides on semiconductors (GeO_2)
3) Comparison with *ab initio* density functional theory and with **<u>k.p theory</u>** (Jose Menendez)
4) Ellipsometry measurements over a broad **spectral range** (30 meV to 9.5 eV) and broad **temperature** range (4 K to 800 K). Also **femtosecond** time resolution (ELI Beamlines).
5) Applications: Microelectronics industry (CMOS, bipolar, III/V), mid-wave infrared detectors

WWW: http://femto.nmsu.edu

Spectroscopic ellipsometry

ellipsometric angles ψ, Δ
refractive index n+ik
dielectric function ε

$$\rho = \frac{r_p}{r_s} = \tan \Psi \, e^{i\Delta}$$

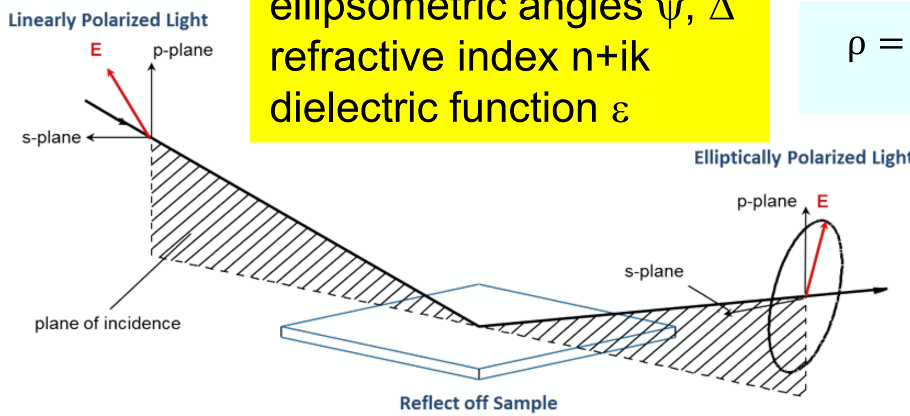

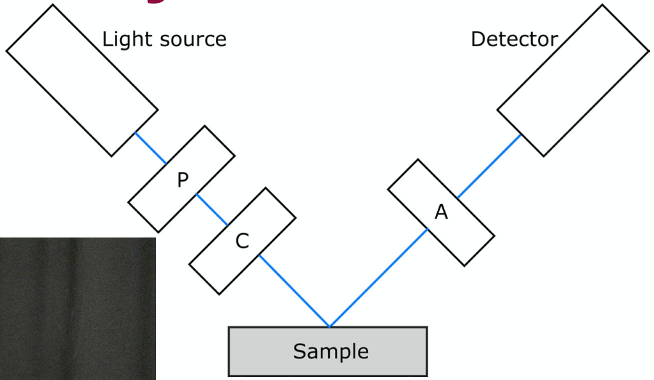

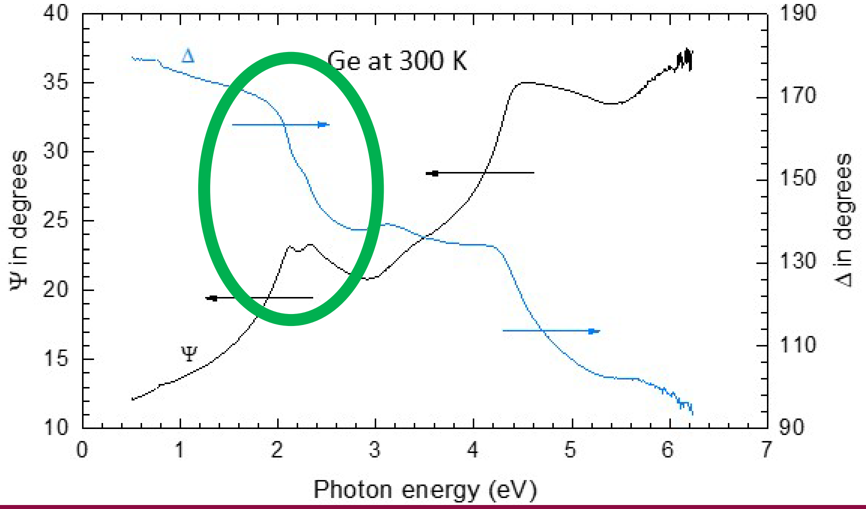

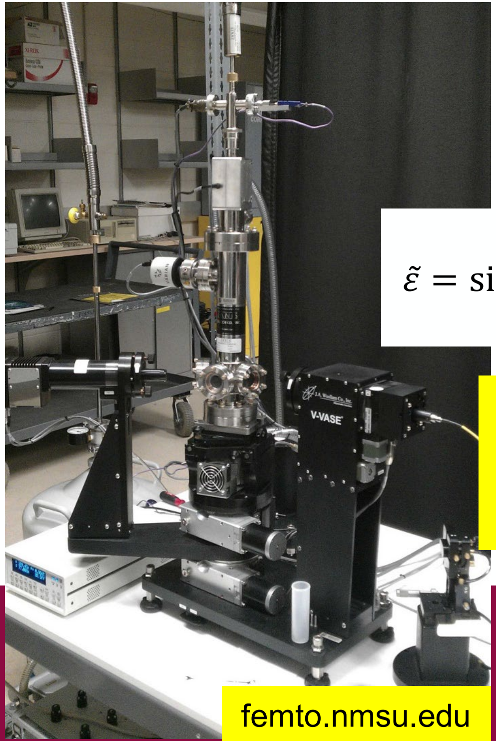

$$\tilde{\varepsilon} = \sin^2 \varphi \left[1 + \tan^2 \varphi \cdot \left(\frac{1-\rho}{1+\rho} \right)^2 \right]$$

UHV cryostat & V-VASE ellipsometer

femto.nmsu.edu

Tompkins & Hilfiker, Spectroscopic Ellipsometry (2016)

Ellipsometry at NMSU

diamond windows
closed-cycle He cooler

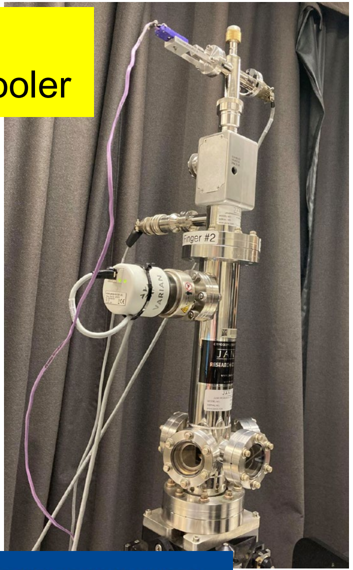

Ellipsometry on anything (inorganic, 3D)

- Metals, insulators, semiconductors
- Mid-IR to vacuum UV (150 nm to 40 μm)
- **10 to 800 K, ultrafast ellipsometry**

Ellipsometry tells us a lot about materials quality (not necessarily what we want to know).

Optical critical points of thin-film $Ge_{1-y}Sn_y$ alloys: A comparative $Ge_{1-y}Sn_y$ / $Ge_{1-x}Si_x$ study VR D'costa, CS Cook, AG Birdwell, CL Littler, M Canonico, S Zollner, ... Physical Review B—Condensed Matter and Materials Physics 73 (12), 125207	445	2006
Growth and strain compensation effects in the ternary $Si_{1-x-y}Ge_xC_y$ alloy system K Eberl, SS Iyer, S Zollner, JC Tsang, FK LeGoues Applied physics letters 60 (24), 3033-3035	397	1992
Ge–Sn semiconductors for band-gap and lattice engineering M Bauer, J Taraci, J Tolle, AVG Chizmeshya, S Zollner, DJ Smith, ... Applied physics letters 81 (16), 2992-2994	341	2002

http://femto.nmsu.edu

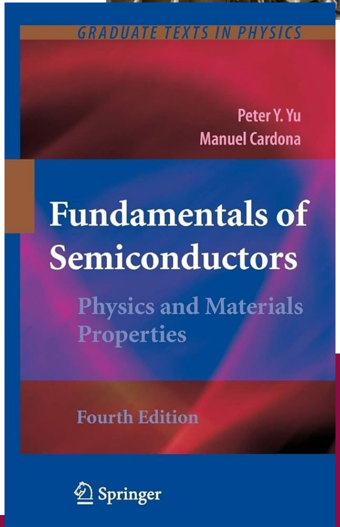

Problem statement: optical constants

(1) Achieve a **quantitative** understanding of **photon absorption** and **emission** processes.

- Our **qualitative** understanding of excitonic absorption is 50-100 years old (Einstein coefficients),
- But **insufficient** for modeling of detectors and emitters.

(2) How are optical processes affected by high carrier concentrations **(screening)**?

- High carrier densities can be achieved with
  - In situ doping (Menendez, Kouvetakis)
  - **high temperatures (narrow-gap or gapless semiconductors)**
  - **ultrafast (femtosecond) lasers**
- **Application:** CMOS-integrated mid-infrared camera (thermal imaging with a phone).

Application: Midwave Infrared Detectors Germanium-Tin Alloys

Intensity of Optical Absorption by Excitons

R. J. Elliott

Phys. Rev. **108**, 1384 – Published 15 December 1957

Article | References | Citing Articles (1,780) | PDF | Export Citation

ABSTRACT

The intensity of optical absorption close to the edge in semiconductors is examined using band theory together with the effective-mass approximation for the excitons. Direct transitions which occur when the band extrema on either side of the forbidden gap are at the same **K**, give a line spectrum and a continuous absorption of characteristically different form and intensity, according as transitions between band states at the extrema are allowed or forbidden. If the extrema are at different **K** values, indirect transitions involving phonons occur, giving absorption proportional to $(\Delta E)^{\frac{1}{2}}$ for each exciton band, and to $(\Delta E)^2$ for the continuum. The experimental results on Cu_2O and Ge are in good qualitative agreement with direct forbidden and indirect transitions, respectively.

Received 9 April 1957

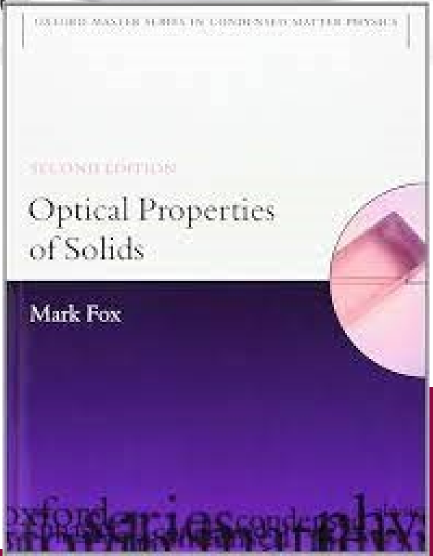

Einstein coefficients

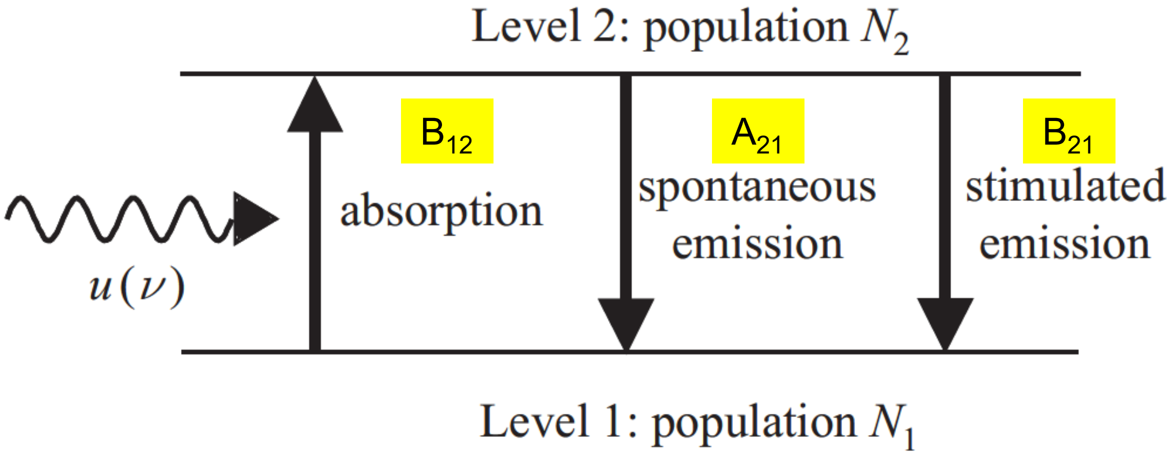

One coefficient is sufficient:

$$g_1 B_{12} = g_2 B_{21}$$

$$A_{21} = \frac{2\hbar\omega^3}{\pi c^3} B_{21}$$

Use Fermi's Golden Rule to calculate B_{12}

In equilibrium: N_1, N_2 constant.
Absorption and emission balance.
Black-body radiation $u(\hbar\omega)$

$$B_{12} N_1 u(\hbar\omega) = A_{21} N_2 + B_{21} N_2 u(\hbar\omega)$$

Albert Einstein, *Strahlungs-Emission und Absorption nach der Quantentheorie*, DPG Verh. **18**, 318 (1916); Phys. Z. **18**, 121 (1917). See also Mark Fox.

Fermi's Golden Rule: Tauc plot

Direct band gap absorption

constant **k·p** matrix element

$$\frac{1}{\tau}=\frac{2\pi}{\hbar}\int_{i,f}|\langle f|H_{eR}|i\rangle|^2\delta(E_f-E_i-\hbar\omega)=\frac{2\pi}{\hbar}|\langle f|H_{eR}|i\rangle|^2 g_{fi}(\hbar\omega)$$

Joint DOS
parabolic bands

$$\langle f|H_{eR}|i\rangle=\frac{e}{m_0}\langle \boldsymbol{f}|\vec{\boldsymbol{p}}|\boldsymbol{i}\rangle\cdot\vec{A}_0$$

Use **k·p** matrix element *P*: $E_P=2P^2/m_0$

$$\varepsilon_2(\hbar\omega)=\frac{e^2\sqrt{m_0}\mu^{\frac{3}{2}}}{3\pi\sqrt{2}\varepsilon_0\hbar}\frac{E_P\sqrt{E_0}}{(\hbar\omega)^2}\sqrt{\frac{\hbar\omega}{E_0}-1}$$

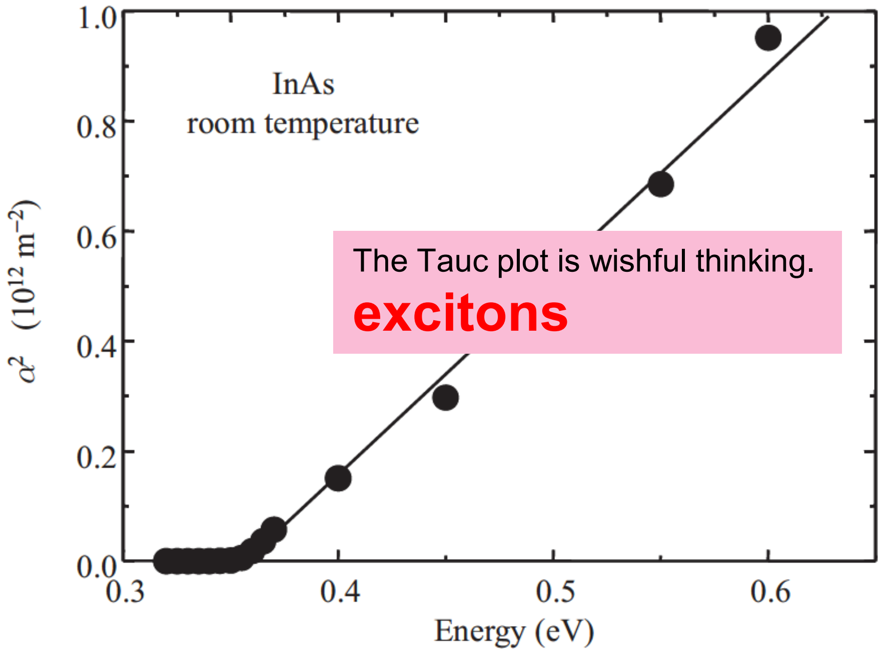

The Tauc plot is wishful thinking.
excitons

Fox, Chapter 3

Fermi's Golden Rule: Tauc plot


Melissa Rivero Arias

Direct band gap absorption

$$\frac{1}{\tau}=\frac{2\pi}{\hbar}\int_{i,f}|\langle f|H_{eR}|i\rangle|^2\delta(E_f-E_i-\hbar\omega)=\frac{2\pi}{\hbar}|\langle f|H_{eR}|i\rangle|^2 g_{fi}(\hbar\omega)$$

$$\langle f|H_{eR}|i\rangle=\frac{e}{m_0}\langle \boldsymbol{f}|\vec{\boldsymbol{p}}|\boldsymbol{i}\rangle\cdot\vec{A}_0$$

Use **k·p** matrix element *P*: $E_P=2P^2/m_0$

$$\varepsilon_2(\hbar\omega)=\frac{e^2\sqrt{m_0}\mu^{\frac{3}{2}}}{3\pi\sqrt{2}\varepsilon_0\hbar}\frac{E_P\sqrt{E_0}}{(\hbar\omega)^2}\sqrt{\frac{\hbar\omega}{E_0}-1}$$

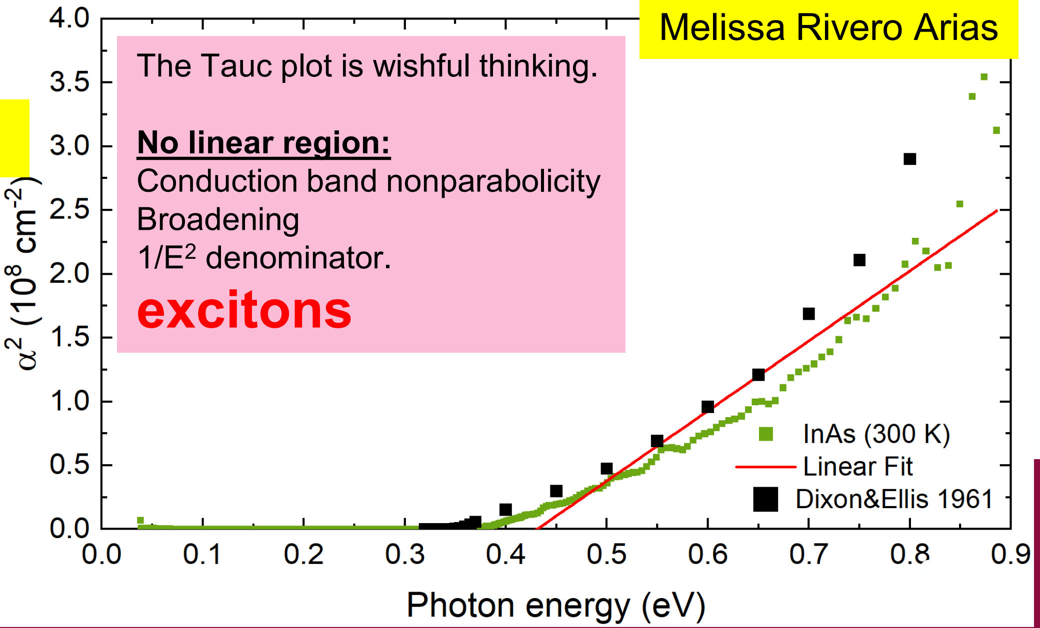

Bohr model for free excitons

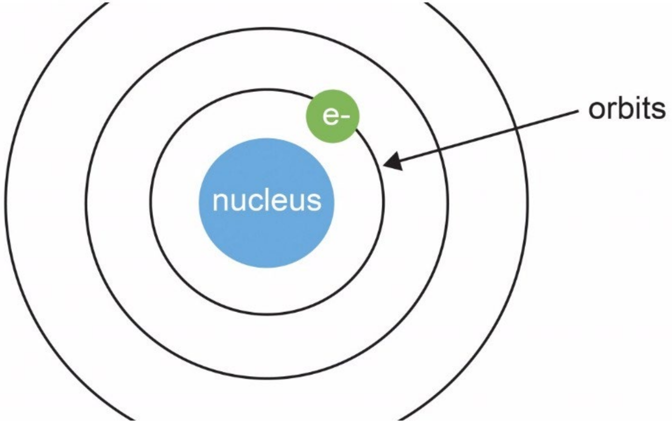

Electron and hole form a bound state with binding energy.

$$E(n) = -\frac{\mu}{m_0}\frac{1}{\varepsilon_r^2}\frac{R_H}{n^2} = -\frac{R}{n^2}$$

R_H=13.6 eV Rydberg energy.
QM mechanical treatment easy.

1. Reduced electron/hole mass (**optical mass**) $$\frac{1}{\mu} = \frac{1}{m_e} + \frac{1}{m_h}$$
2. **Static screening** with static dielectric constant ε_r.
3. **Exciton radius**: $$a_n = \frac{m_0}{\mu}\varepsilon_r n^2 a_H$$
   a_H=0.53 Å
4. Excitons **stable** if R>>kT
5. Exciton **momentum** is zero.
6. **Exciton enhancement important even if R<<kT (high temperature).**

Sommerfeld enhancement (3D)

Excitonic Rydberg energy

$$R = \frac{\mu}{m_0 \varepsilon_r^2} R_H$$

Discrete states

$$E_n = E_g - \frac{1}{n^2} R_X$$

Discrete absorption

$$\varepsilon_2(E) = \frac{8\pi |P|^2 \mu^3}{3\omega^2 (4\pi\varepsilon_0)^3 \varepsilon_r^3} \sum_{n=1}^{\infty} \frac{1}{n^3} \delta(E - E_n)$$

Continuum absorption

$$\varepsilon_2(E) = \frac{2|P|^2 (2\mu)^{3/2} \sqrt{E - E_0}}{3\omega^2} \frac{\xi e^{\xi}}{\sinh \xi}$$

$$\xi = \pi \sqrt{R / E - E_0}$$

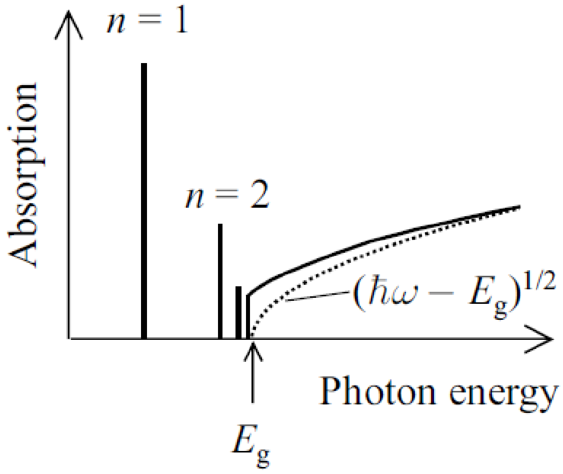

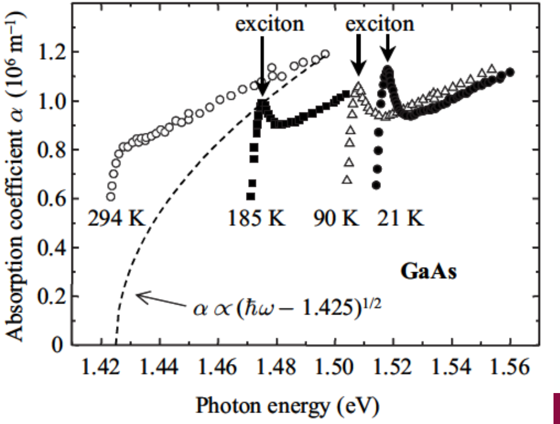

Use Bohr wave functions to calculate ε_2.
Toyozawa discusses broadening.

R. J. Elliott, Phys. Rev. **108**, 1384 (1957)
Yu & Cardona; Fox, Chapter 4; Tanguy 1995

Elliott-Tanguy exciton absorption

Direct band gap absorption

Excitonic binding energy: $R = R_H \times \mu_h / \varepsilon_s^2$

$$\varepsilon_2(\hbar\omega) = \frac{e^2\sqrt{m_0}\mu^{\frac{3}{2}}}{3\pi\sqrt{2}\varepsilon_0\hbar}\frac{E_P\sqrt{R}}{(\hbar\omega)^2}\left[\sum_{n=1}^{\infty}\frac{4\pi R}{n^3}\delta\left(\hbar\omega - E_0 + \frac{R}{n^2}\right) + \frac{2\pi H(\hbar\omega - E_0)}{1 - \exp\left(-2\pi\sqrt{R/\hbar\omega - E_0}\right)}\right]$$

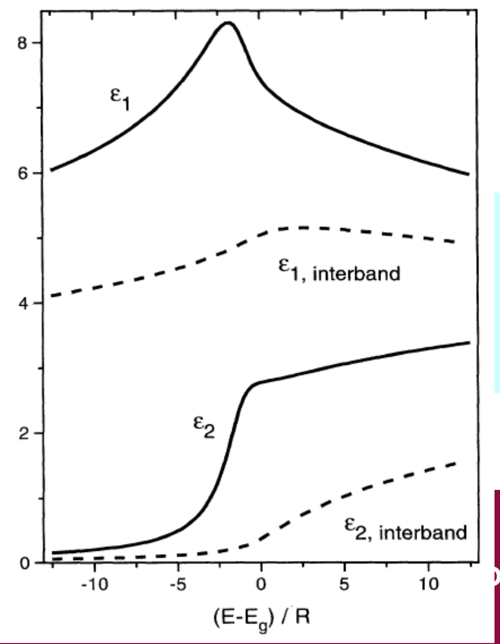

bound excitons

exciton continuum enhancement

Tanguy’s contributions:

- Add Lorentzian broadening
- Kramers-Kronig transform to get the real part.

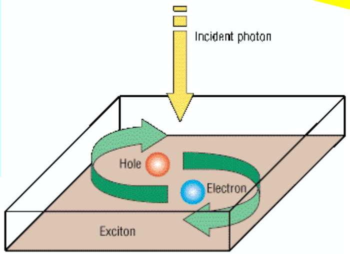

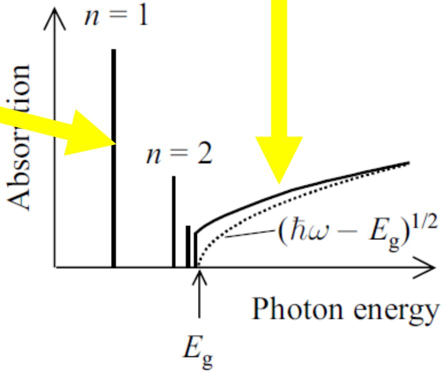

R. J. Elliott, Phys. Rev. **108**, 1384 (1957).
Christian Tanguy, Phys. Rev. Lett. **75**, 4090 (1995) + (E)

Intensity of Optical Absorption by Excitons

R. J. Elliott
Phys. Rev. **108**, 1384 – Published 15 December 1957

Article | References | Citing Articles (1,780) | PDF | Export Citation

ABSTRACT

The intensity of optical absorption close to the edge in semiconductors is examined using band theory together with the effective-mass approximation for the excitons. Direct transitions which occur when the band extrema on either side of the forbidden gap are at the same **K**, give a line spectrum and a continuous absorption of characteristically different form and intensity, according as transitions between band states at the extrema are allowed or forbidden. If the extrema are at different **K** values, indirect transitions involving phonons occur, giving absorption proportional to $(\Delta E)^{\frac{1}{2}}$ for each exciton band, and to $(\Delta E)^2$ for the continuum. The experimental results on Cu_2O and Ge are in good qualitative agreement with direct forbidden and indirect transitions, respectively.

Received 9 April 1957

Elliott-Tanguy theory applied to Ge

- **Fixed parameters:**
- Electron and hole masses (temperature dependent)
- Excitonic binding energy R
- Amplitude A (derived from matrix element P)

- **Adjustable parameters:**
- Broadening Γ: 2.3 meV
- Band gap E_0
- Linear background A_1 and B_1 (contribution from E_1 to real part of ε)

- **Problems:**
- Broadening below the gap (band tail, oxide correction)

Quantitative agreement

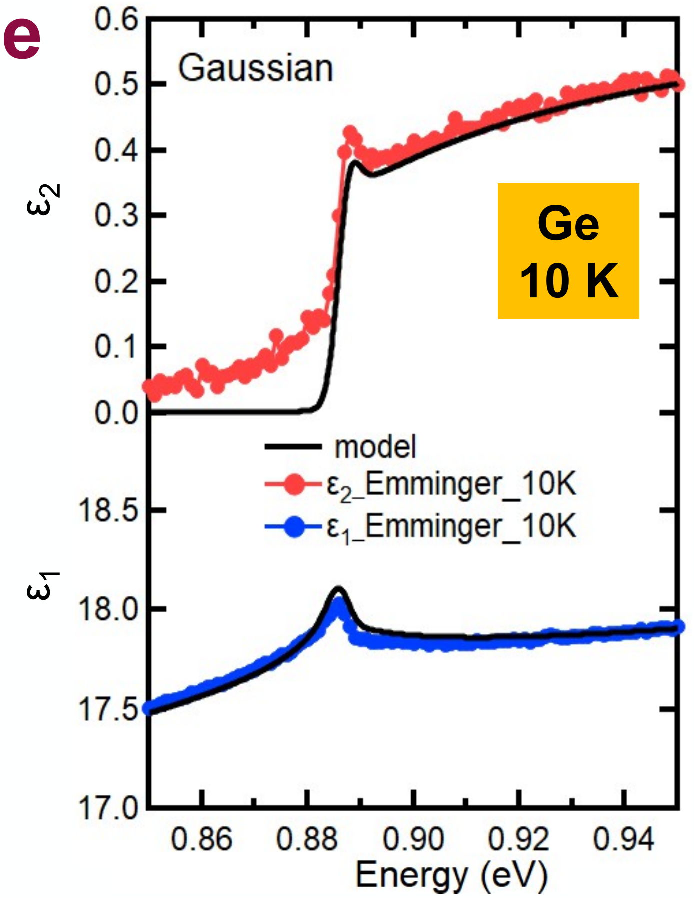

Carola Emminger *et al.*, JAP **131**, 165701 (2022).

Elliott-Tanguy theory applied to Ge

Good agreement at low temperatures.

Model also describes second derivatives.

Potential problems:

- Matrix element k-dependent
- Nonparabolicity
- Resonant indirect absorption
- ??? at high T.

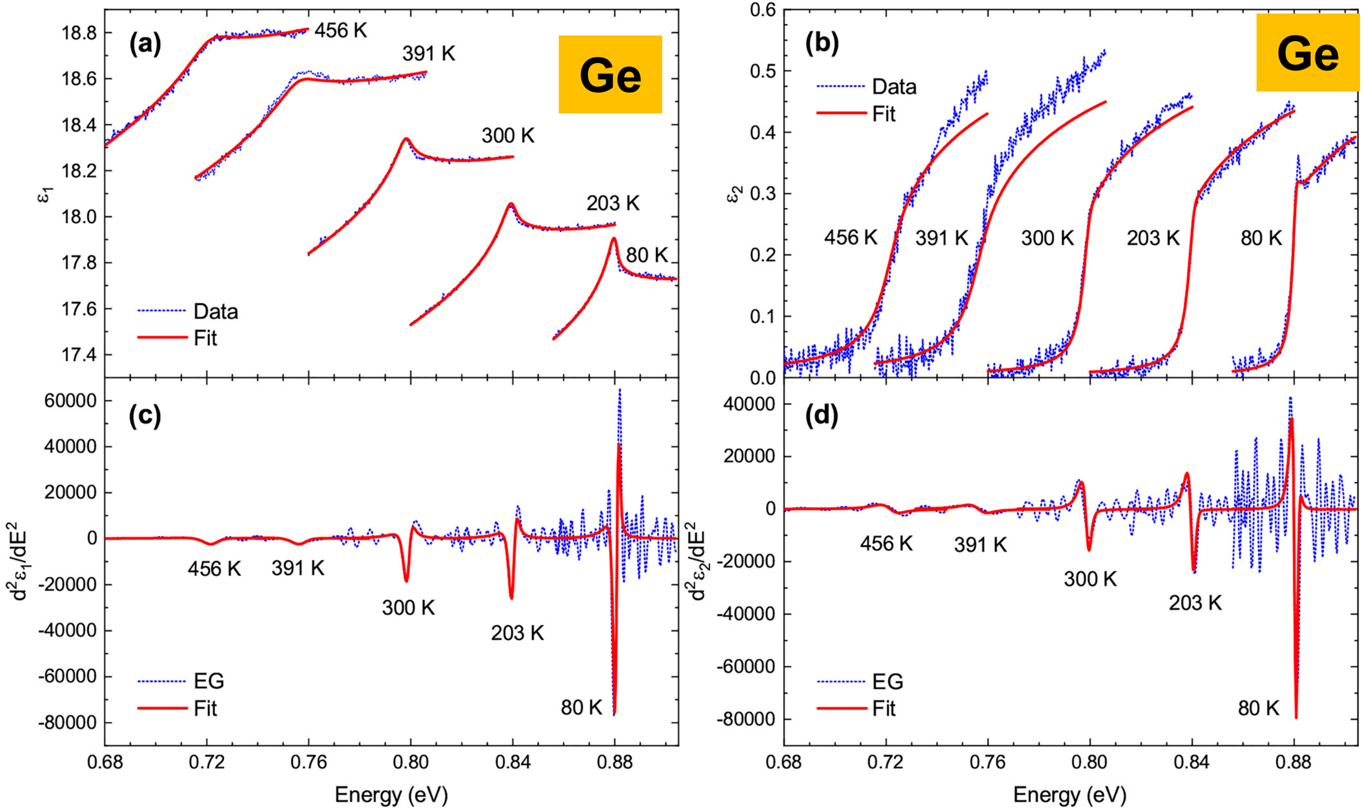

Carola Emminger *et al.*, JAP **131**, 165701 (2022).

Elliott-Tanguy theory: problems for Ge at high T

Good agreement at low temperatures.

Model also describes second derivatives.

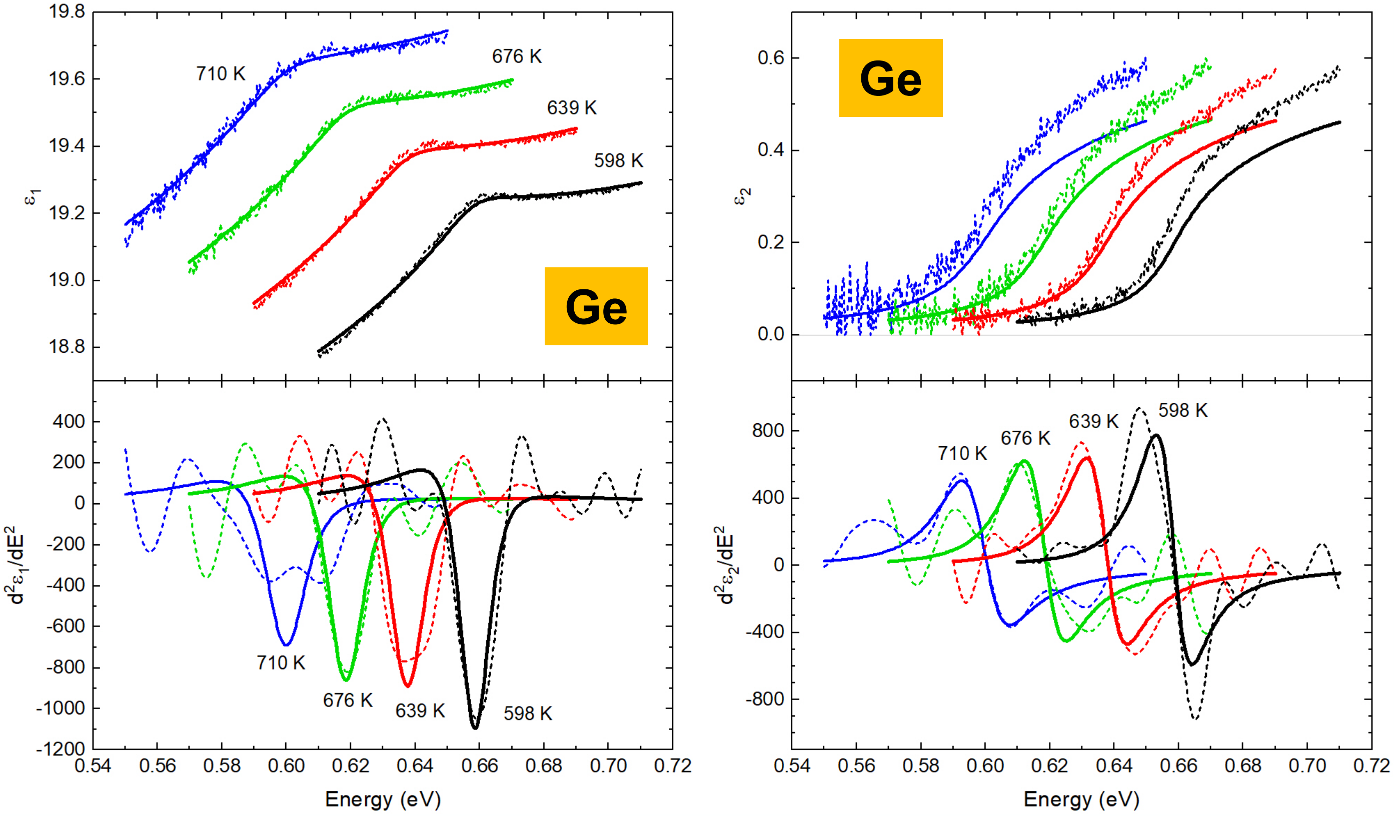

Potential problems:

- Matrix element k-dependent
- Nonparabolicity
- Resonant indirect absorption
- **Temperature dependence of the effective mass.**

Temperature dependence of the effective mass

- Effective electron mass given by k·p theory

$$\frac{1}{m_e(T)} = 1 + \frac{E_P}{3}\left(\frac{2}{E_0(T)} + \frac{1}{E_0(T)+\Delta_0}\right)$$

E_0: direct band gap
k·p matrix element P: $E_P = 2P^2/m_0$

- Temperature dependence of the direct band gap has two contributions:
  - Thermal expansion of the lattice
  - Electron-phonon interaction (Debye-Waller term and self-energy)
- "Mass band gap" should **only include the thermal expansion**.

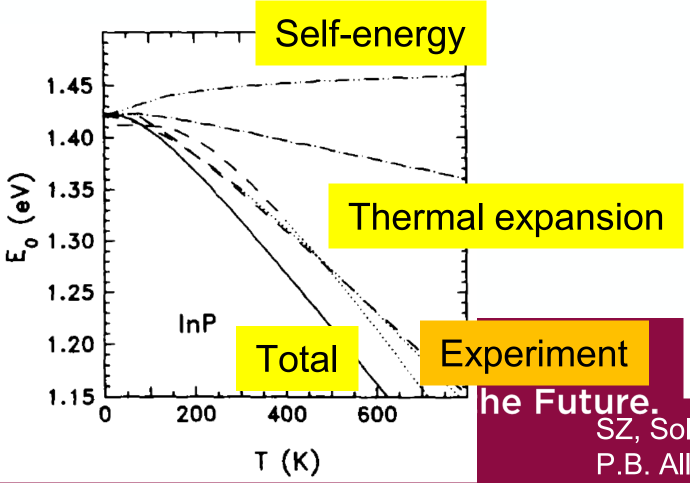

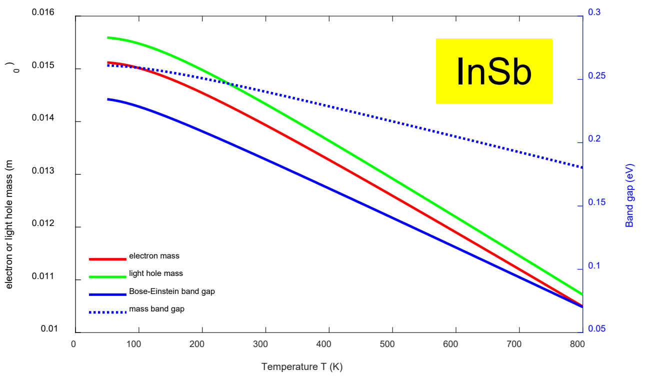

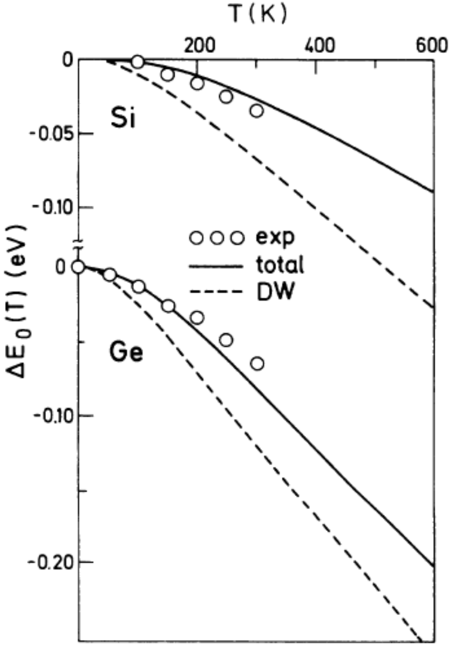

he Future.

SZ, Solid State Commun. **77**, 485 (1991).
P.B. Allen and M. Cardona, Phys. Rev. B **27** 4760 (1983).

Two-dimensional saddle-point excitons (E_1, $E_1+\Delta_1$)

$$\varepsilon(E) = \frac{A}{(E+i\Gamma)^2}\{g[\xi(E+i\Gamma)] + g[\xi(-E-i\Gamma)] - 2g[\xi(0)]\}$$

$$g(\xi) = 2\ln(\xi) - 2\psi(\frac{1}{2} - \xi)$$

$$\psi(z) = \frac{d\ln\Gamma(z)}{dz}$$

$$\xi(z) = \sqrt{{}^{R}/_{E_0} - z}$$

$$A = \frac{\mu e^2}{3\pi\varepsilon_0 m_0^2}|P|^2$$

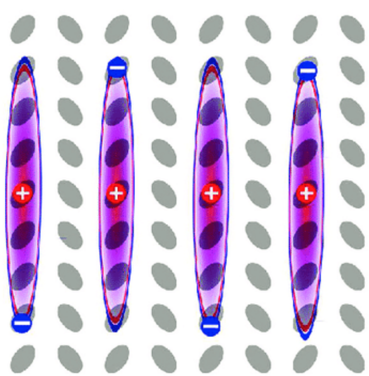

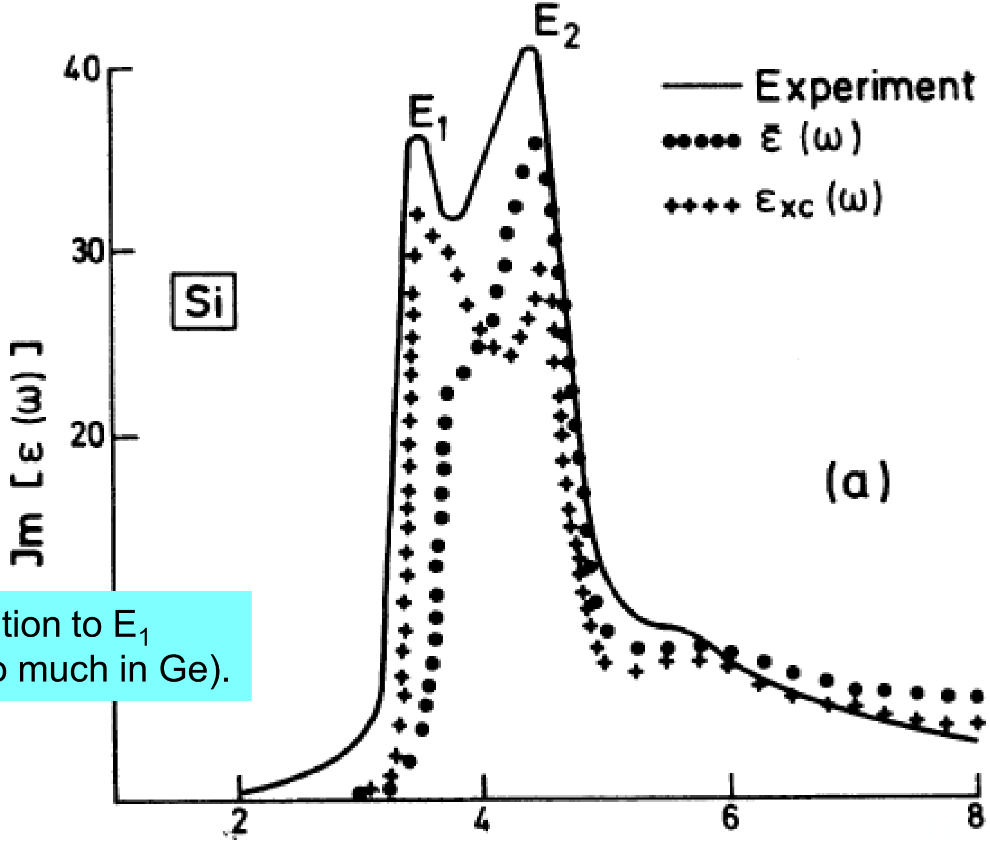

Strong excitonic contribution to E_1 critical point in Si (mot so much in Ge).

B. Velicky and J. Sak, phys. status solidi **16**, 147 (1966)
W. Hanke and L.J. Sham, Phys. Rev. B **21**, 4656 (1980)
C. Tanguy, Solid State Commun. 98, 65 (1996)

Two-dimensional Bohr problem

$$H=-\frac{\hbar^2}{2\mu_\perp}\left(\frac{\partial^2}{\partial x^2}+\frac{\partial^2}{\partial y^2}\right)-\frac{\hbar^2}{2\mu_\parallel}\frac{\partial^2}{\partial z^2}-\frac{e^2}{\varepsilon_r r}$$

Assume that $\mu_{||}$ along (111) is infinite (separate term).
Use cylindrical coordinates.
Separate radial and polar variables.
Similar Laguerre solution as 3D Bohr problem.

$$a_X=\frac{\varepsilon_r m_0}{\mu_\perp}a_H \qquad R=\frac{\mu_\perp}{m_0\varepsilon_r^2}R_H$$

(same as in 3D)

$$E_n=-\frac{R}{\left(n-\frac{1}{2}\right)^2},\qquad n=1,2,\ldots$$

Half-integral quantum numbers

2D critical point

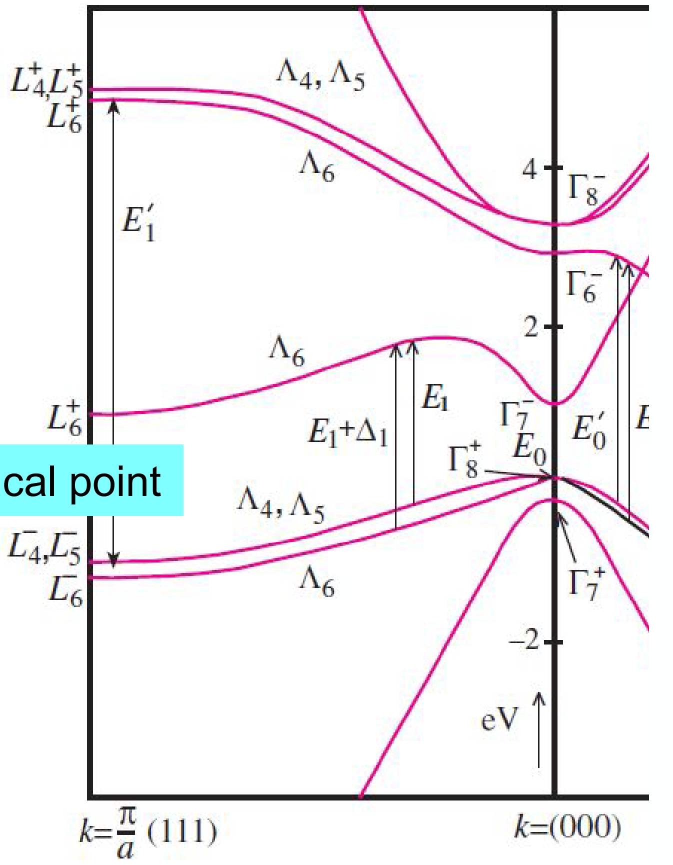

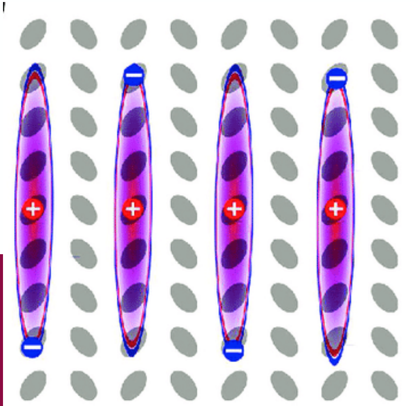

M. Shinada and S. Sugano, J. Phys. Soc. Jpn. **21**, 1936 (1966).
Flügge (Rechenmethoden QM, 1952).

Two-dimensional excitons at E_1 critical points of Ge

$$\varepsilon(E) = \frac{k_{max} e^2 \bar{P}^2 \mu_\perp^{(E_1)}}{3\varepsilon_0 m^2 \pi (E + i\Gamma)^2} \left\{ g_a \left[\sqrt{\frac{R}{E_g - (E + i\Gamma)}} \right] + g_a \left[\sqrt{\frac{R}{E_g - (-E - i\Gamma)}} \right] - 2 g_a \left[\sqrt{\frac{R}{E_g - (0)}} \right] \right\}$$

with

$$g_a(\xi) = 2\ln\xi - 2\psi(\xi)$$

Peak at $n = 0$ for $E_g - 4R$

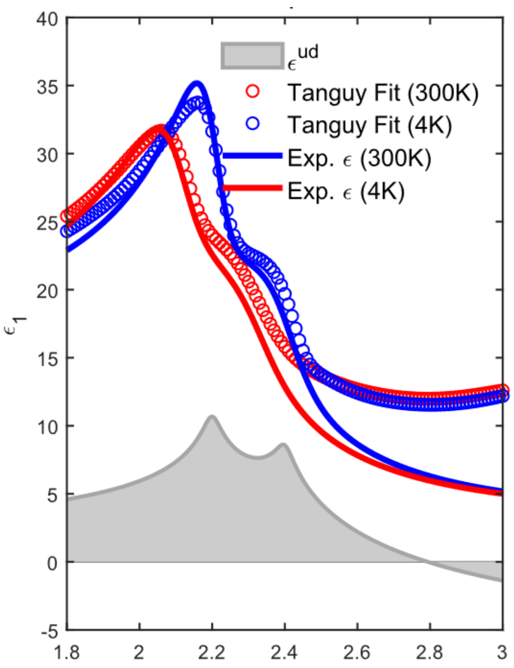

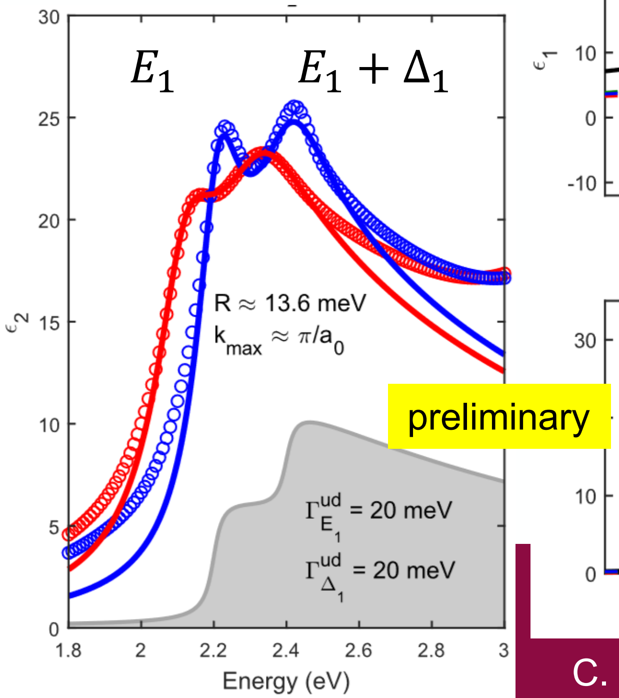

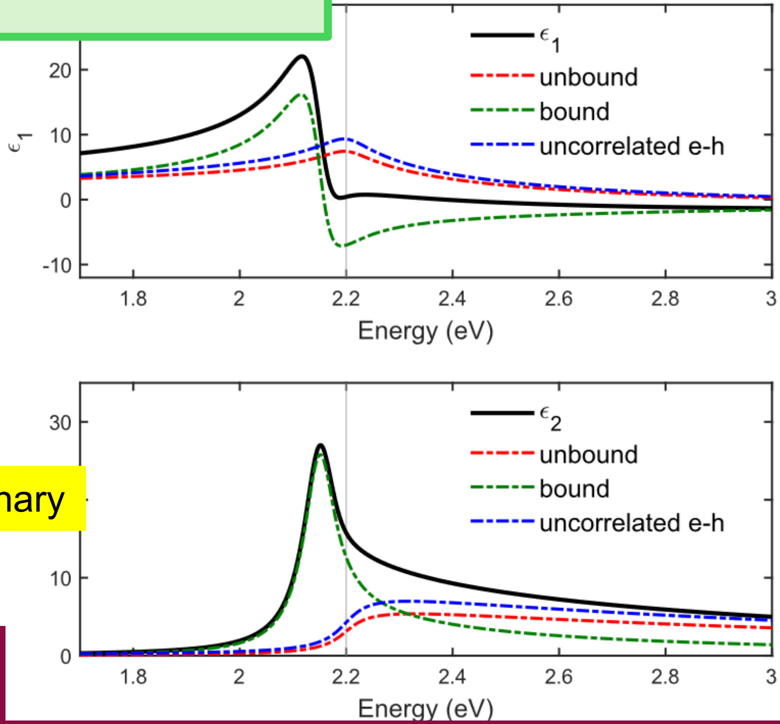

C. Tanguy, SSC **98**, 65 (1996).

Problem statement: optical constants

*(1) Achieve a **quantitative** understanding of **photon absorption** and **emission** processes.*

- *Our **qualitative** understanding of excitonic absorption is 50-100 years old (Einstein coefficients),*
- *But **insufficient** for modeling of detectors and emitters.*

(2) How are optical processes affected by **high carrier concentrations** (screening)?

- High carrier densities can be achieved with
  - In situ doping (Menendez, Kouvetakis; Arizona State University)
  - **high temperatures (narrow-gap or gapless semiconductors)**
  - **ultrafast (femtosecond) lasers**
- **Application:** CMOS-integrated mid-infrared camera (thermal imaging with a phone).

Condensation of excitons at high density

Exciton gas

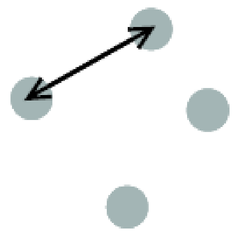

(a) Low density
Separation $\gg$ diameter

Electron-hole liquid

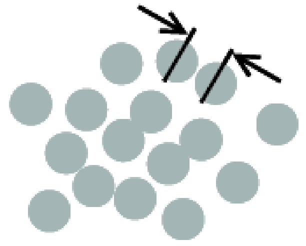

(b) High density
Separation $\approx$ diameter

Mott transition (insulator-metal) when electron separation equals exciton radius.

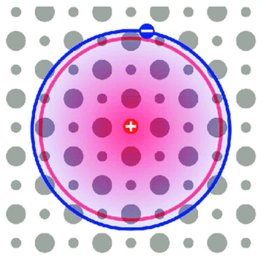

Electron separation d for density N

$$d = \sqrt[3]{\frac{3}{4\pi n}}$$

$$r_s = \frac{d}{a_X}$$

dimensionless

Mott transition occurs at r_s near 1.
GaAs: $n=10^{17}$ cm^{-3}.

Biexciton, triexciton molecule formation.
Electron-hole droplets. Bose-Einstein condensation.

Fox, Chapter 4

Excitons in doped or excited semiconductors

Need to include exciton screening due to doping.
Yukawa potential: Schrödinger equation not solvable.
Use Hulthen potential as an approximation

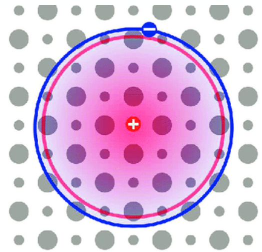

Coulomb $$V(r) = -k\frac{1}{r}$$ $$k = \frac{e^2}{4\pi\varepsilon_0\varepsilon_r}$$

Yukawa $$V(r) = -k\frac{\exp(-r/\lambda_\mathrm{D})}{r}$$ $$\lambda_D = \sqrt{\frac{\varepsilon_r\varepsilon_0 k_B T}{ne^2}} = \frac{1}{k_D}$$

Debye screening length

Hulthen $$V(r) = -k\frac{2/ga_X}{\exp\left(\frac{2r}{ga_X}\right) - 1}$$ $$g = \frac{\lambda_D}{a_X}$$

Unscreened: g=∞
Fully screened: g=0
Mott criterion: g=1

Hulthen exciton

e Future.

C. Tanguy, Phys. Rev. **60,** 10660 (1999).
Banyai & Koch, Z. Phys. B **63**, 283 (1986). Haug & Koch (2009).

Tanguy: Dielectric function of screened excitons

Bound exciton states (finite number):

$$A = \frac{\hbar^2 e^2}{6\pi\varepsilon_0 m_0^2}\left(\frac{2\mu}{\hbar^2}\right)^{3/2} |P|^2$$

$$\varepsilon_2(\omega) = \frac{2\pi A\sqrt{R}}{E^2}\sum_{n=1}^{n^2<g} 2R\frac{1}{n}\left(\frac{1}{n^2}-\frac{n^2}{g^2}\right)\delta\left[E-E_0+\frac{R}{n^2}\left(1-\frac{n^2}{g}\right)^2\right]$$

Reduced Rydberg energy

exciton continuum:

$$\varepsilon_2(\omega) = \frac{2\pi A\sqrt{R}}{E^2}\frac{\sinh \pi g k}{\cosh(\pi g k)-\cosh\left(\pi g\sqrt{k^2-\frac{4}{g}}\right)}\theta(E-E_0)$$

$$k = \pi\sqrt{{(E-E_0)}/{R}}$$

Need to introduce Lorentzian broadening and perform numerical KK transform.

C. Tanguy, Phys. Rev. B **60**, 10660 (1999)

Tanguy: Dielectric function of screened excitons

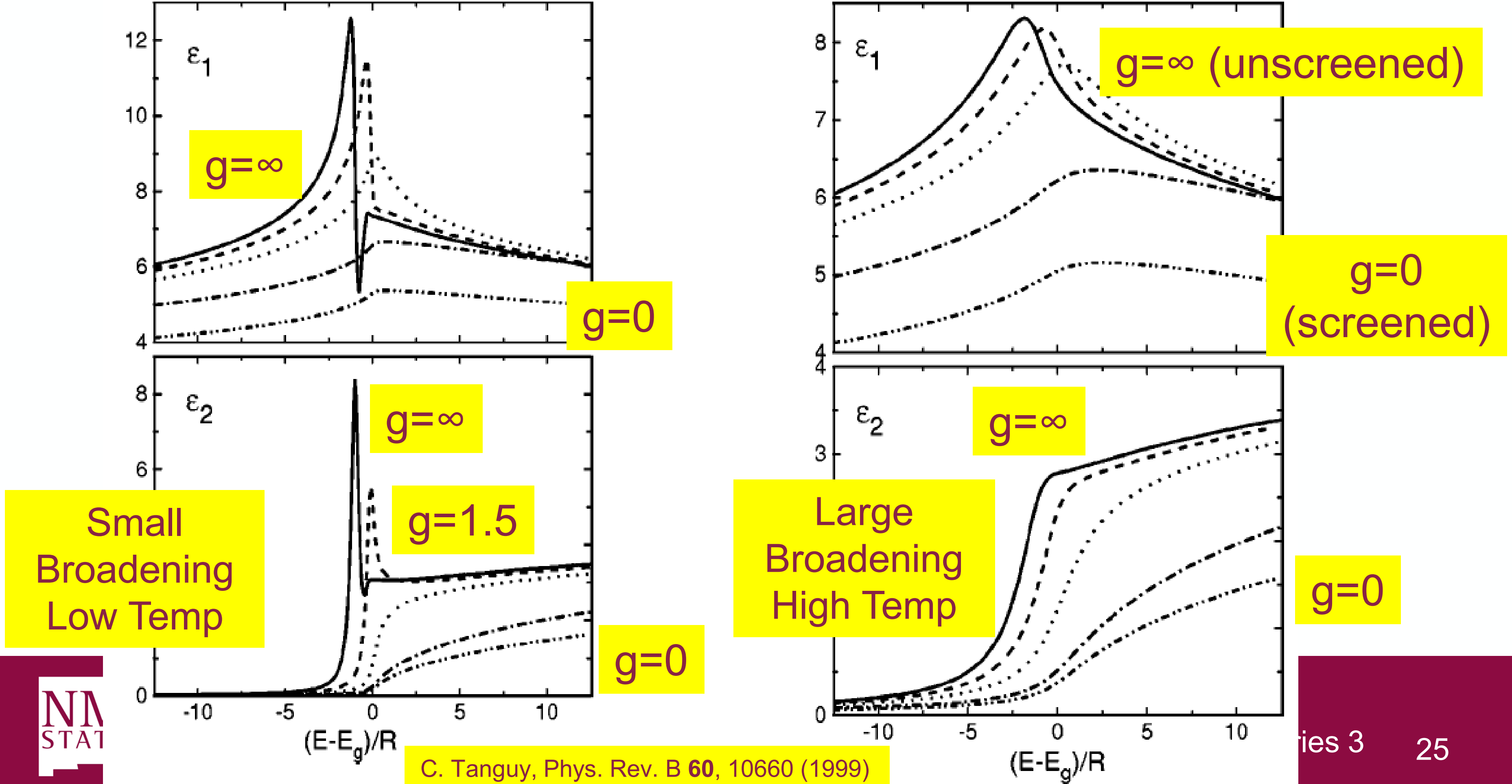

C. Tanguy, Phys. Rev. B **60**, 10660 (1999)

k·p theory (band structure method)

Schrödinger equation

$$H\Phi_{n\vec{k}} = \left(\frac{\vec{p}^2}{2m_0} + V\right)\Phi_{n\vec{k}} = E_{n\vec{k}}\Phi_{n\vec{k}}$$

Use Bloch's theorem:

$$\Phi_{n\vec{k}}(\vec{r}) = e^{i\vec{k}\cdot\vec{r}} u_{n\vec{k}}(\vec{r})$$

Product rule

$$(fg)'' = f''g + 2f'g' + fg''$$

Solve equation for **k**=0.

$$\left(\frac{\vec{p}^2}{2m_0} + \frac{\hbar^2\vec{\boldsymbol{k}}^2}{2\boldsymbol{m_0}} + \frac{\hbar\vec{\boldsymbol{k}}\cdot\vec{\boldsymbol{p}}}{\boldsymbol{m_0}} + V\right)u_{n\vec{k}} = E_{n\vec{k}}u_{n\vec{k}}$$

Eliminate green free-electron term with substitution of variables (Kane 1957).

Then treat red term in perturbation theory.

Works very well for semiconductors with local V(**r**) potentials.

Yu & Cardona, Fundamentals of Semiconductors
Kane, J. Phys. Chem. Solids **1**, 249 (1957). Kane 1966.

Relativistic Effects: Darwin Shift: C, Si, Ge, Sn

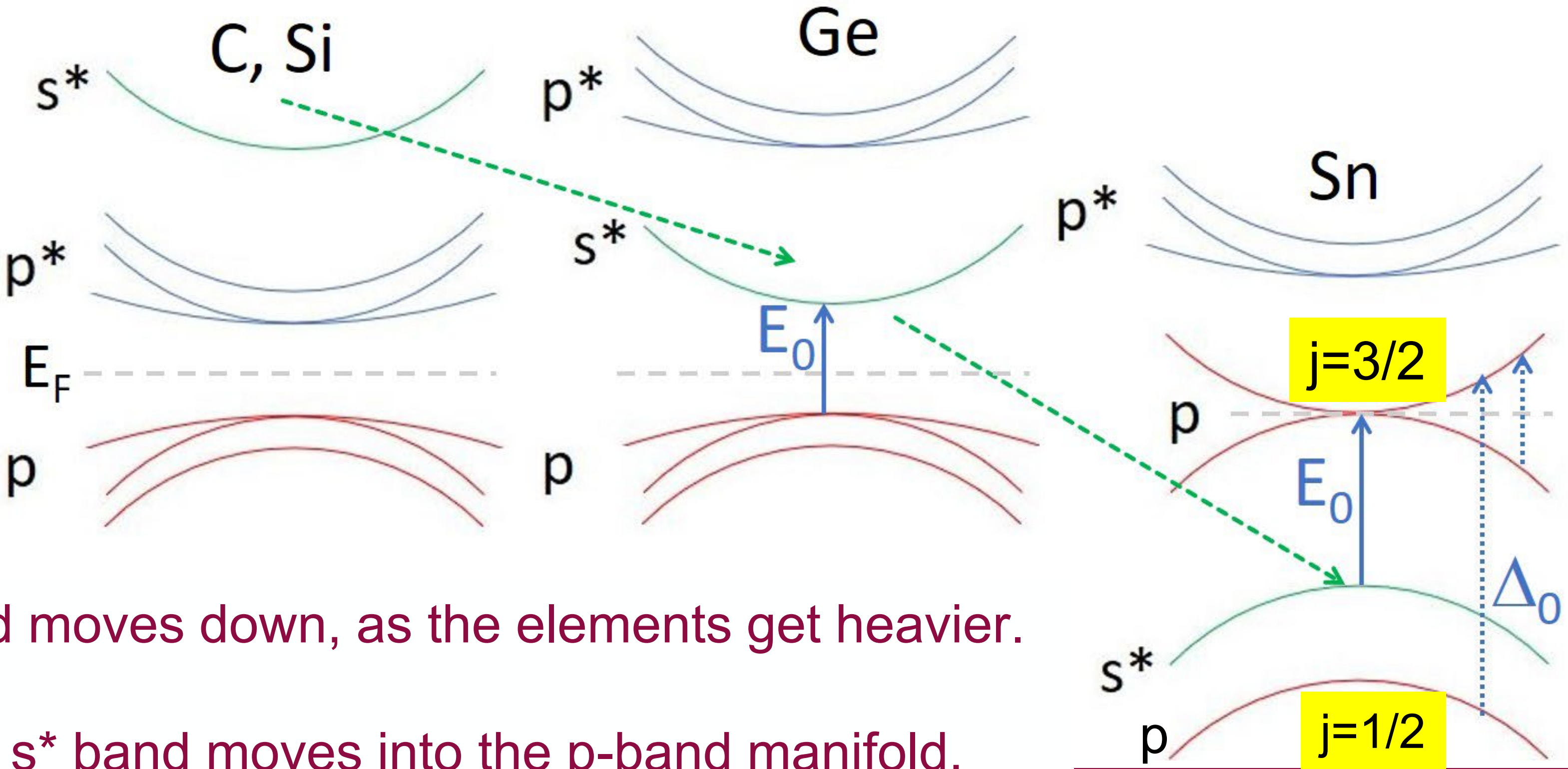

The s* band moves down, as the elements get heavier.

In α-tin, the s* band moves into the p-band manifold, between the j=1/2 and j=3/2 states.
This makes α-tin an (**inverted**) **gapless** semiconductor.

Intravalence band absorption in gapless topological insulators (α-tin)

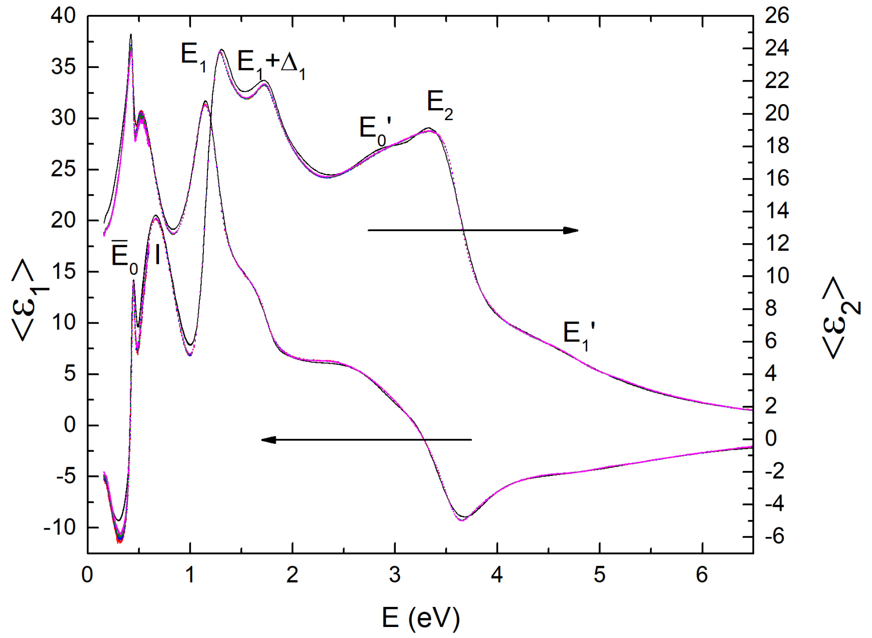

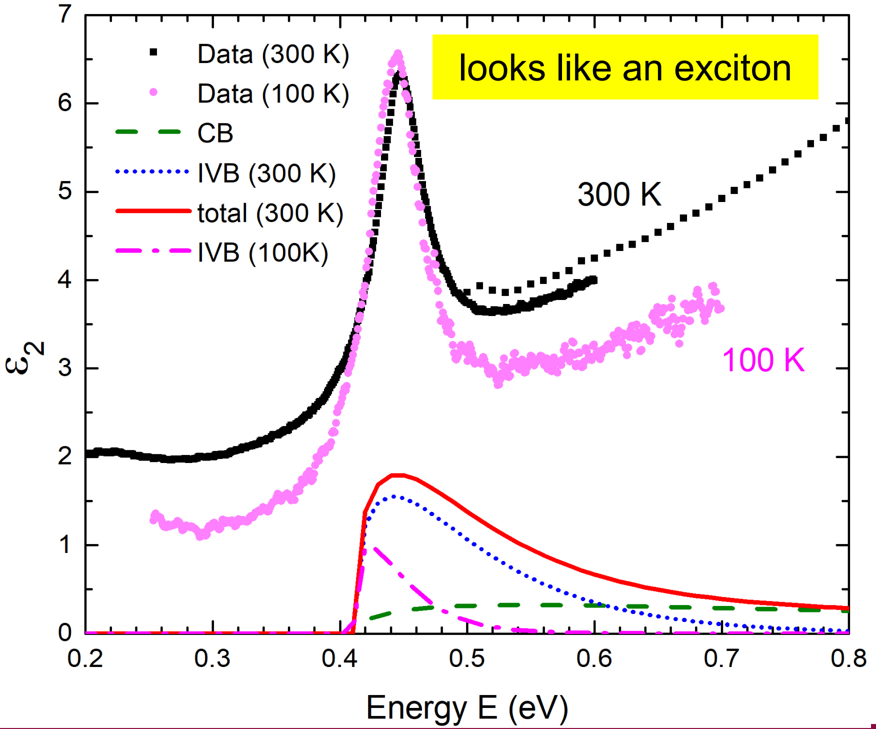

R.A. Carrasco, APL **113**, 232104 (2018).

All gapless (inverted) semiconductors should have this peak.
Theory with same model as Ge IVB (Kaiser 1953, Kahn 1955).

Simple 8x8 k·p band structure of α-tin (Kane)

Kane 8x8 k·p Hamiltonian:

$$\tilde{H}_{\vec{k}} = \begin{pmatrix} E_0 & 0 & -\frac{\hbar\vec{k}}{m_0} iP & 0 \\ 0 & -\frac{2\Delta_0}{3} & \frac{\sqrt{2}\Delta_0}{3} & 0 \\ \frac{\hbar\vec{k}}{m_0} iP & \frac{\sqrt{2}\Delta_0}{3} & -\frac{\Delta_0}{3} & 0 \\ 0 & 0 & 0 & 0 \end{pmatrix}$$

Cubic characteristic equation:

$$\tilde{E}\left(\tilde{E} - E_0\right)\left(\tilde{E} + \Delta_0\right) - \frac{\hbar^2 k^2 E_P}{2m_0}\left(\tilde{E} + \frac{2\Delta_0}{3}\right) = 0$$

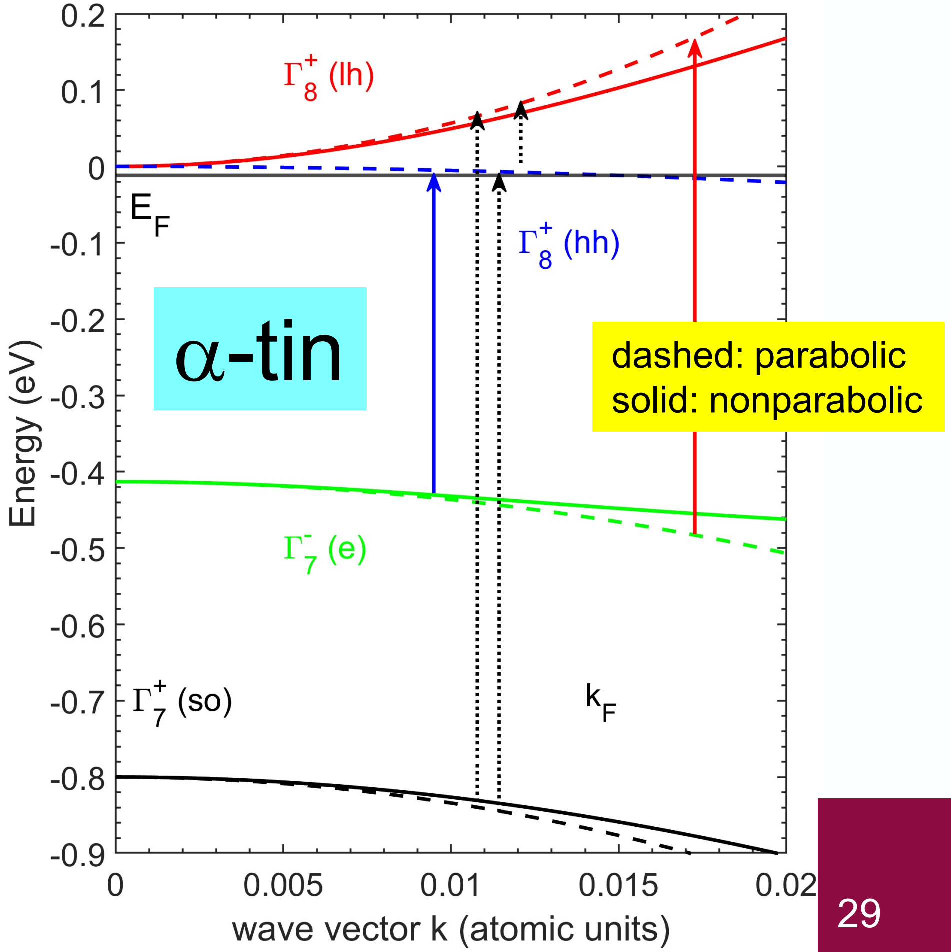

S. Zollner, JVST B **42**, 022203 (2024).

e.

Excitonic intravalence band absorption in α-tin

Parabolic bands

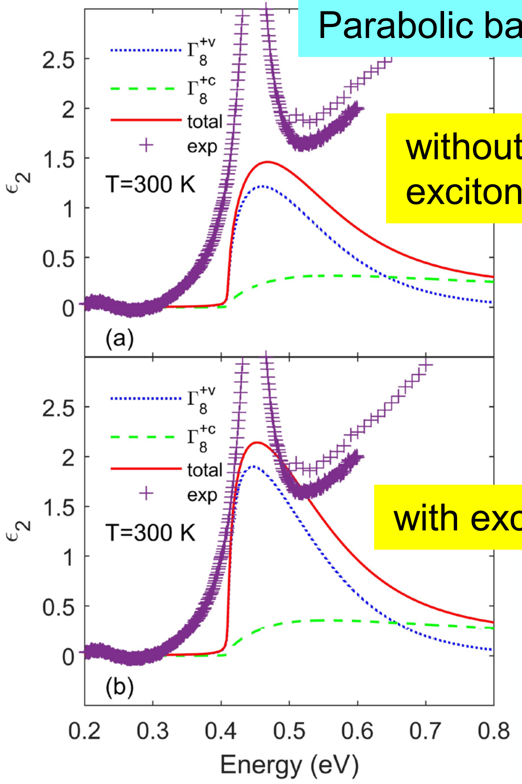

without excitons

with excitons

Screening:

$$r_s = \frac{1}{a_x}\sqrt[3]{\frac{3}{4\pi n}}$$

$$V(r) = -k\frac{\exp(-r/\lambda_D)}{r}$$

$$\lambda_D = \sqrt{\frac{\varepsilon_r \varepsilon_0 k_B T}{pe^2}} = \frac{1}{k_D}$$

nonparabolicity affects exciton radius (screening)

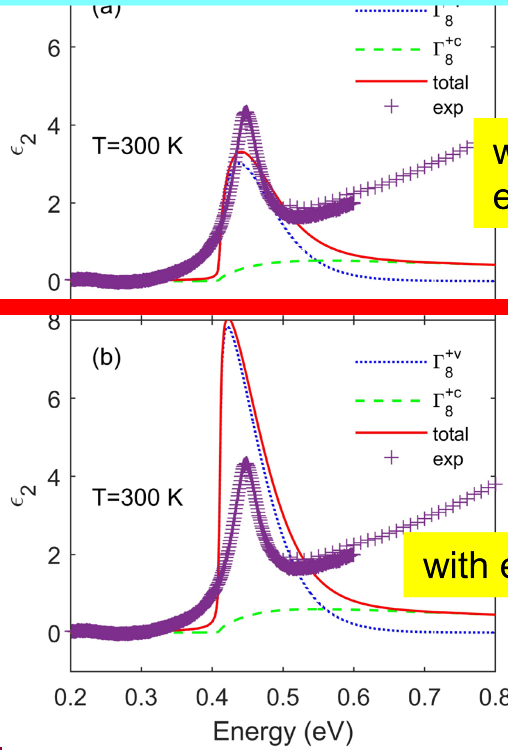

without excitons

with excitons

S. Zollner, JVST B **42**, 022203 (2024).

Dielectric function of InSb from 80 to 800 K

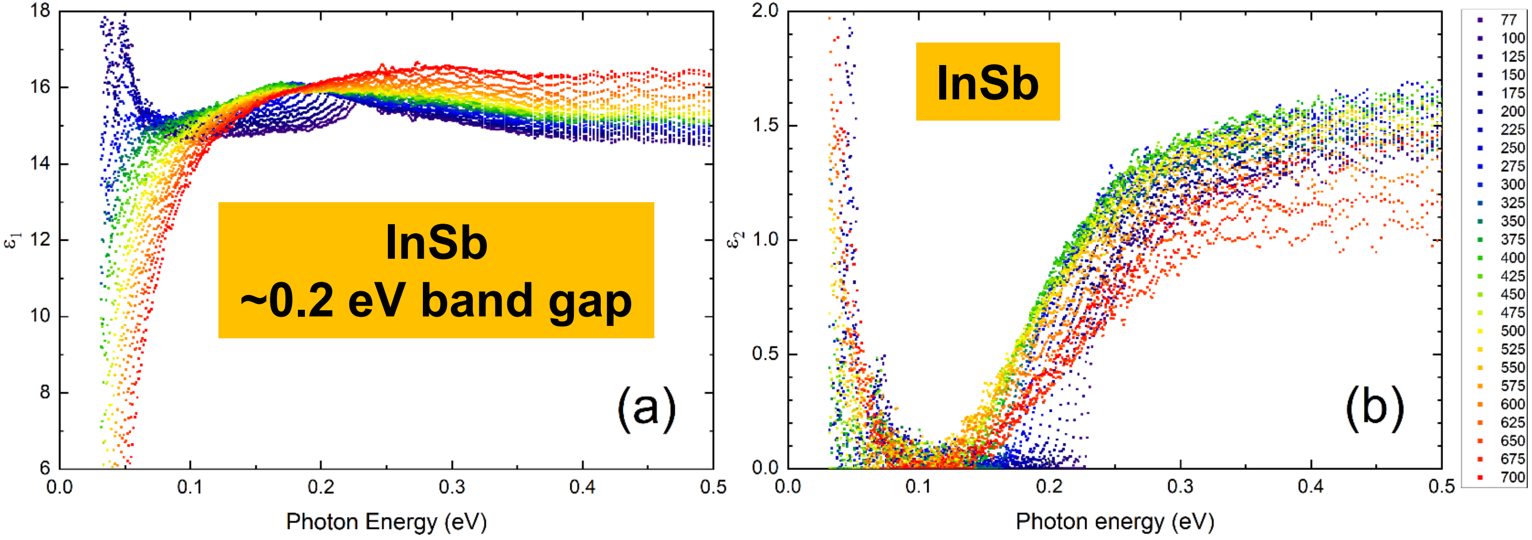

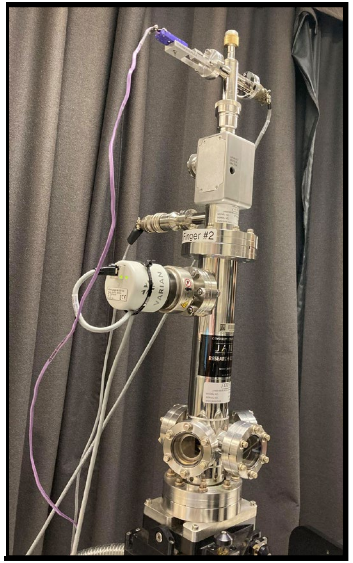

Woollam FTIR-VASE cryostat with CVD diamond windows

- **Band gap** changes with temperature (but only below 500 K).
- **Amplitude reduction at high temperatures (Pauli blocking, bleaching)**
- **Drude response** at high temperatures (thermally excited carriers).
- Depolarization artifacts at long wavelengths (below 300 K).

Optical constants model: screened excitons

$$\varepsilon_2(E)=\frac{2\pi A\sqrt{R}}{E^2}\left\{\sum_{n=1}^{\sqrt{g}}\frac{2R}{n}\left(\frac{1}{n^2}-\frac{n^2}{g^2}\right)\delta\left[E-E_0+\frac{R}{n^2}\left(1-\frac{n^2}{g}\right)^2\right]+\frac{\sinh(\pi gk)\mathrm{H}(E-E_0)}{\cosh(\pi gk)-\cosh\left(\pi g\sqrt{k^2-\frac{4}{g}}\right)}\right\}[f_h(E)-f_e(E)]$$

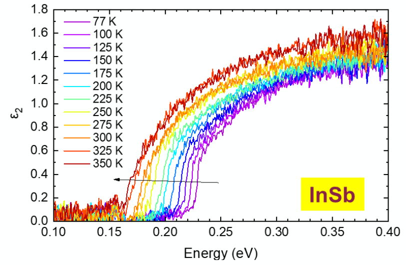

- **Absorption by screened excitons** (Hulthen potential)
- **Degenerate Fermi-Dirac statistics** to calculate f_h and f_e.
- Numerical Kramers-Kronig transform (need occupation factors)
- Two terms for light and heavy excitons
- **Non-parabolicity and temperature-dependent mass** included from k.p theory
- **k-dependent matrix element *P*.**
- Screening parameter $g=12/\pi^2 a_R k_{TF}$ (large: no screening)
  Sommerfeld enhancement persists well above the Mott density.
- **Only two free parameters: Band gap E_0 and broadening Γ**
- Amplitude *A* and exciton binding energy *R* from k.p theory and effective masses

Christian Tanguy, Phys. Rev. B **60**, 10660 (1999).
Jose Menendez, Phys. Rev. B **101**, 195204 (2020).
Carola Emminger, J. Appl. Phys. **131**, 165701 (2022).

Band gap analysis for InSb

How does the band gap of InSb change with temperature?

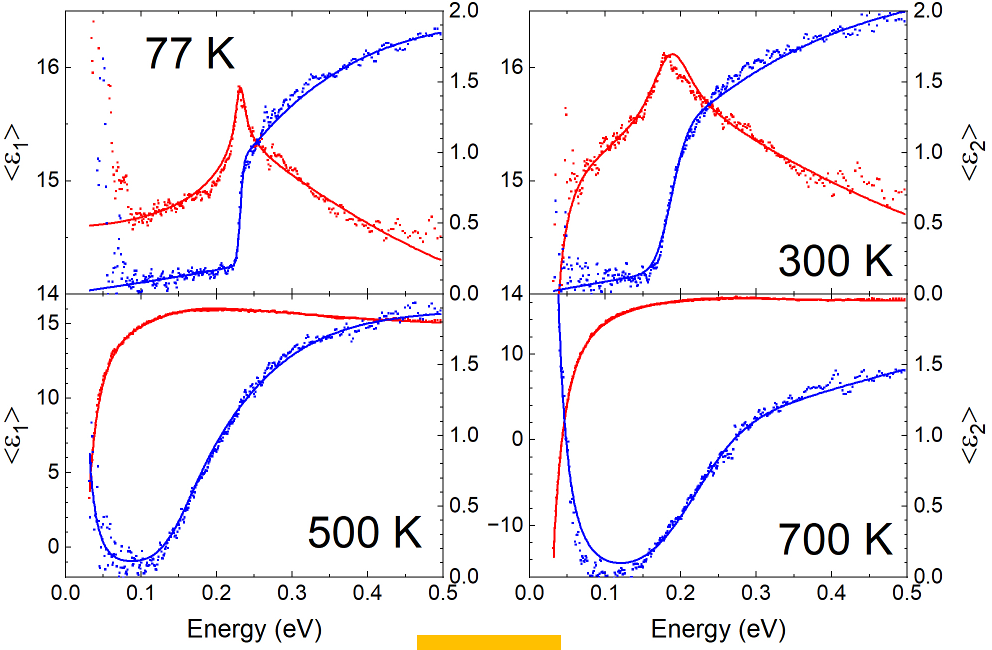

Parametric-Semiconductor Model:

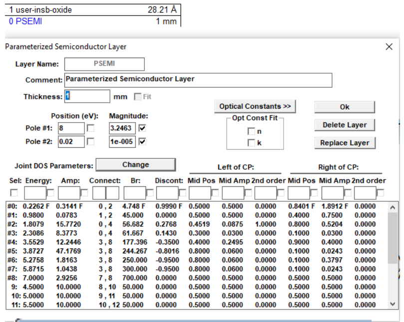

Fit

	Final
MSE	0.2958
En0.0	0.22615 ± 0.000889
Br0.0	4.7478 ± 1.32
Am0.0	0.31415 ± 124
Disc0.0	0.999 ± 788
RPos0.0	0.84009 ± 0.0264
RAmp0.0	1.8912 ± 0.191
PoleMag.0	3.2469 ± 6.56
PoleMag2.0	1e-005 ± 0.000568

Also vary “shape parameters”.

Asymmetric peak shape poorly described.

Try Tanguy oscillator for excitonic line shape.

C. M. Herzinger, B. Johs, et al., J. Appl. Phys. **83**, 3323 (1998)
Melissa Rivero Arias, JVSTB **41**, 022203 (2023)

Band gap of InSb from 80 to 800 K

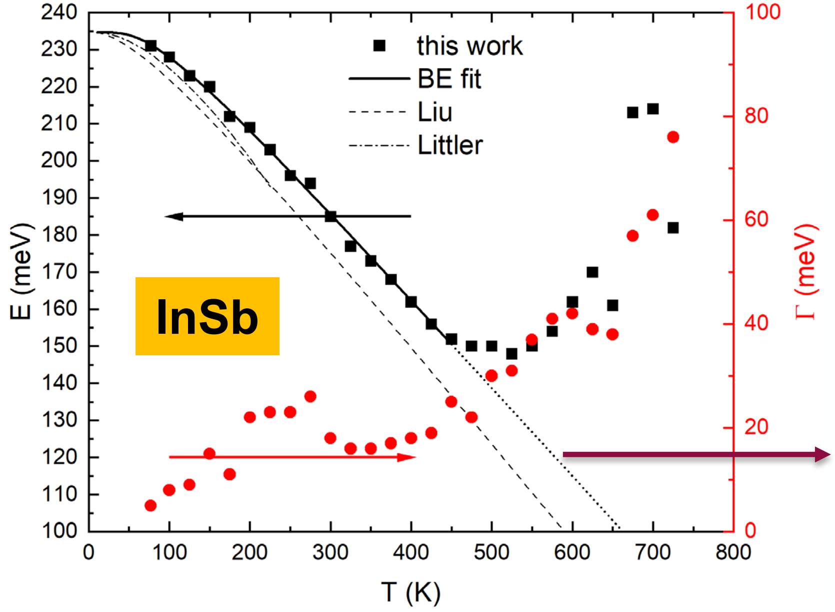

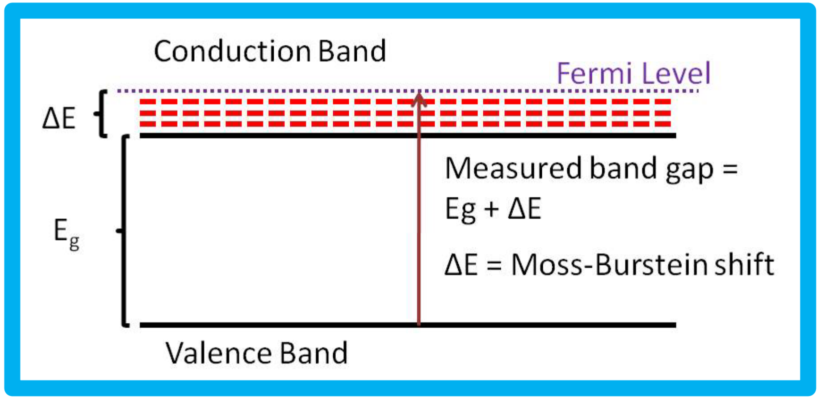

Bose-Einstein Model

$$E_0(T) = E^{\text{un}} - b\left[1 + \frac{2}{\exp\left(\Omega/k_B T\right)}\right]$$

- Band gap changes with temperature (but only below 500 K)
- Described by Bose-Einstein model below 500 K: Logothetidis, PRB **31**, 947 (1985).
- No redshift above 500 K: **Thermal Burstein-Moss shift**

T.S. Moss, Proc. Phys. Soc. **67**, 775 (1954).
E. Burstein, Phys. Rev. **93**, 632 (1954).

Nonparabolicity of InSb conduction band from k·p theory

Kane 8x8 k·p Hamiltonian:

$$\tilde{H}_{\vec{k}} = \begin{pmatrix} E_0 & 0 & -\frac{\hbar\vec{k}}{m_0}iP & 0 \\ 0 & -\frac{2\Delta_0}{3} & \frac{\sqrt{2}\Delta_0}{3} & 0 \\ \frac{\hbar\vec{k}}{m_0}iP & \frac{\sqrt{2}\Delta_0}{3} & -\frac{\Delta_0}{3} & 0 \\ 0 & 0 & 0 & 0 \end{pmatrix}$$

Cubic characteristic equation:

$$\tilde{E}(\tilde{E}-E_0)(\tilde{E}+\Delta_0) - \frac{\hbar^2 k^2 E_P}{2m_0}\left(\tilde{E}+\frac{2\Delta_0}{3}\right) = 0$$

Large spin-orbit approximation:

$$E_{3,4} = \frac{\hbar^2 k^2}{2m_0} + \frac{E_0}{2}\left(1 \pm \sqrt{1+\frac{\hbar^2 k^2}{2m_0}\frac{2}{\mu_{lh}E_0}}\right)$$

Kane, J. Phys. Chem. Solids **1**, 249 (1957).

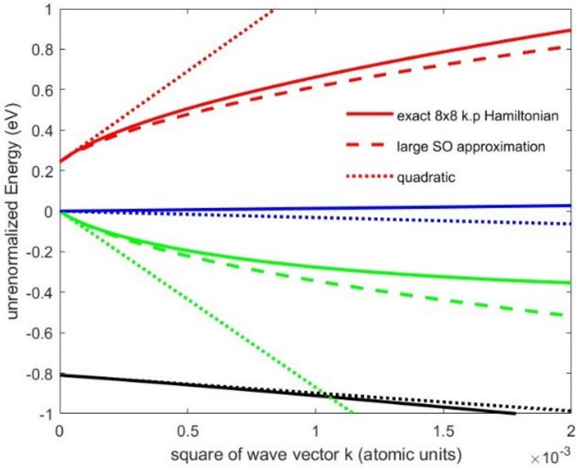

Energy versus k (InSb)

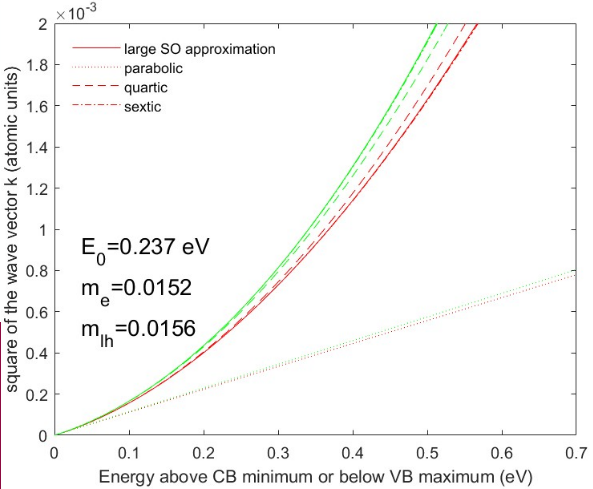

Density of CB states

$$\frac{\hbar^2 k^2}{2m_0 m^*} = \varepsilon(1+\alpha\varepsilon+\beta\epsilon^2)$$

$$\alpha = \frac{(1-m^*)^2}{E_0}$$

Femtosecond Pump-Probe Ellipsometry

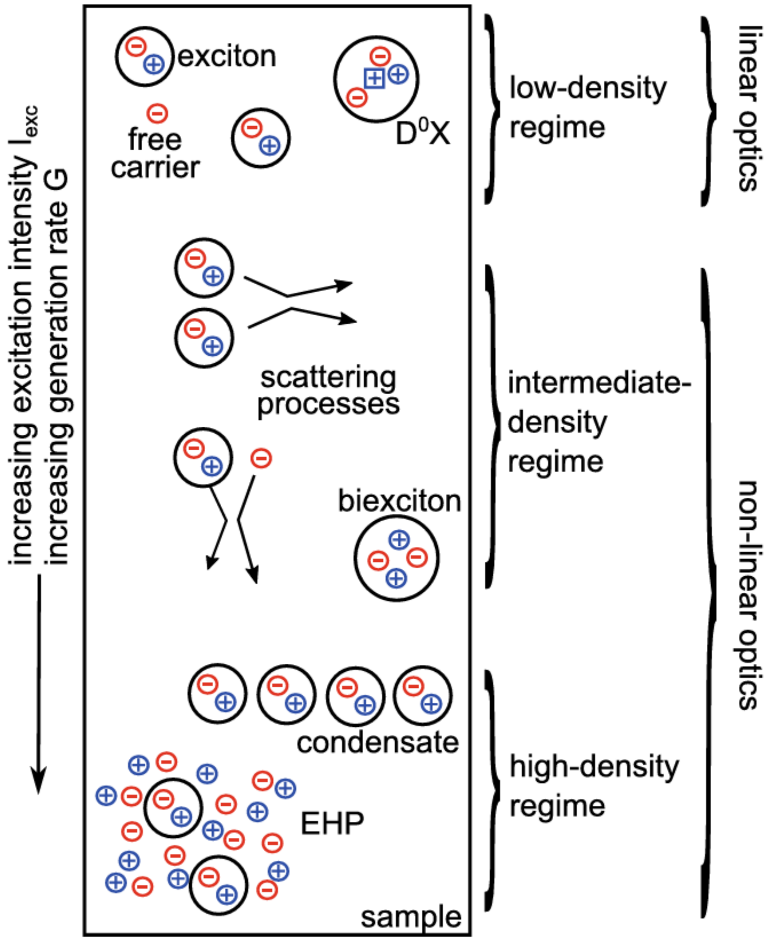

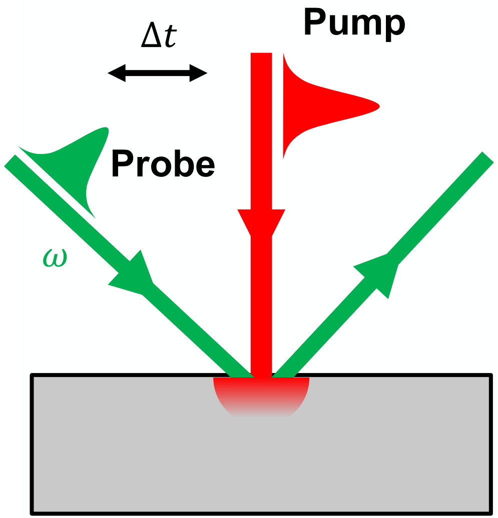

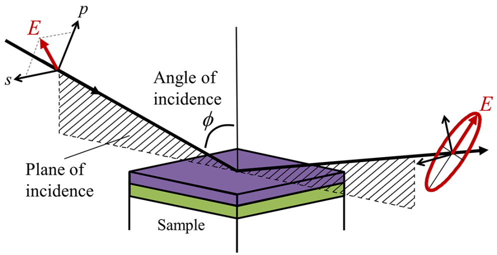

Non-linear effects in germanium induced by photoexcited carriers:

- Screening (many-body)
- Carrier-carrier scattering.
- Carrier-phonon scattering.
- Intervalley scattering.
- Momentum and energy relaxation of hot carriers.

H. Kalt, Semiconductor Optics 2 (2024).
Tompkins & Hilfiker, Spectroscopic Ellipsometry (2016)

Experimental setup: pump-probe ellipsometry

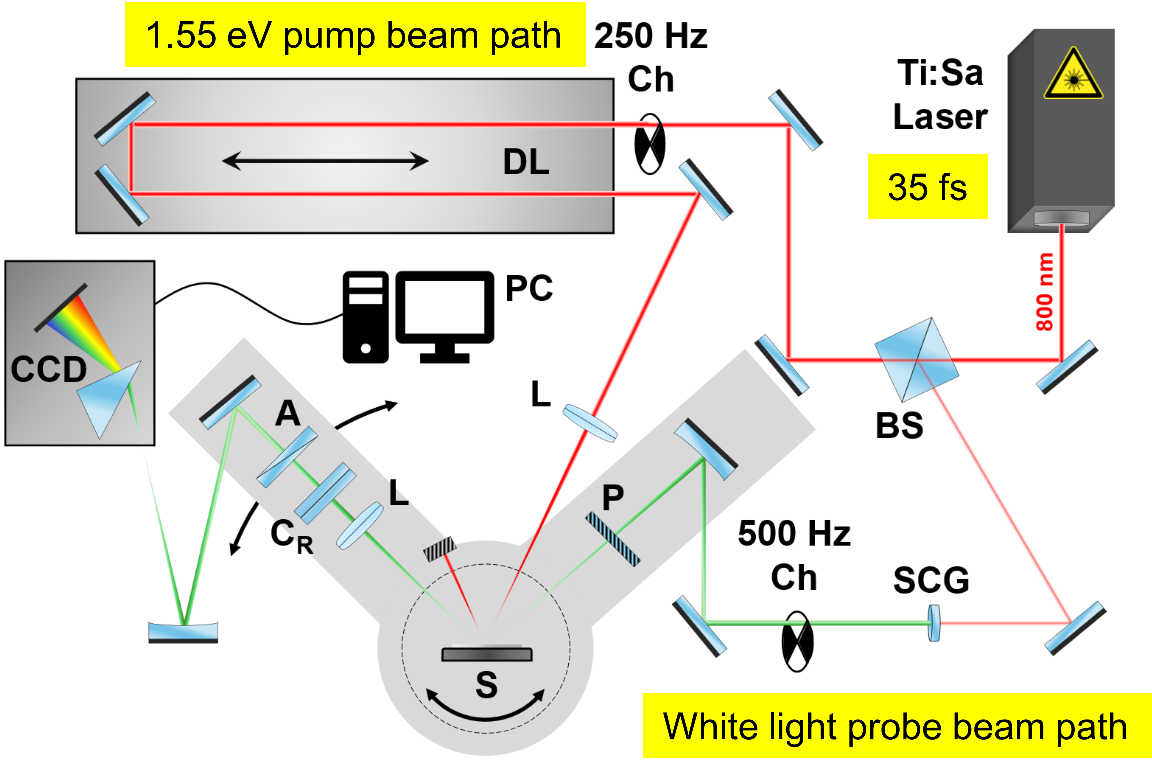

Ch: Chopper (500 Hz, 250 Hz)

A: Analyzer

P: Polarizer

C_R: Rotating Compensator

L: Lens

S: Sample

DL: Delay Line
(~6.67 ns pump-probe delay, 3 fs resolution)

BS: Beam Splitter

SCG: Super-continuum Generation

CCD: Charge-coupled device detector

Eli Beamlines
Dolni Brezany, Czech Republic

S. Richter, Rev. Sci. Instrum. **92**, 033104 (2021).
S. Espinoza, Appl. Phys. Lett. **115**, 052105 (2019).

Set-up: Femtosecond pump-probe ellipsometry

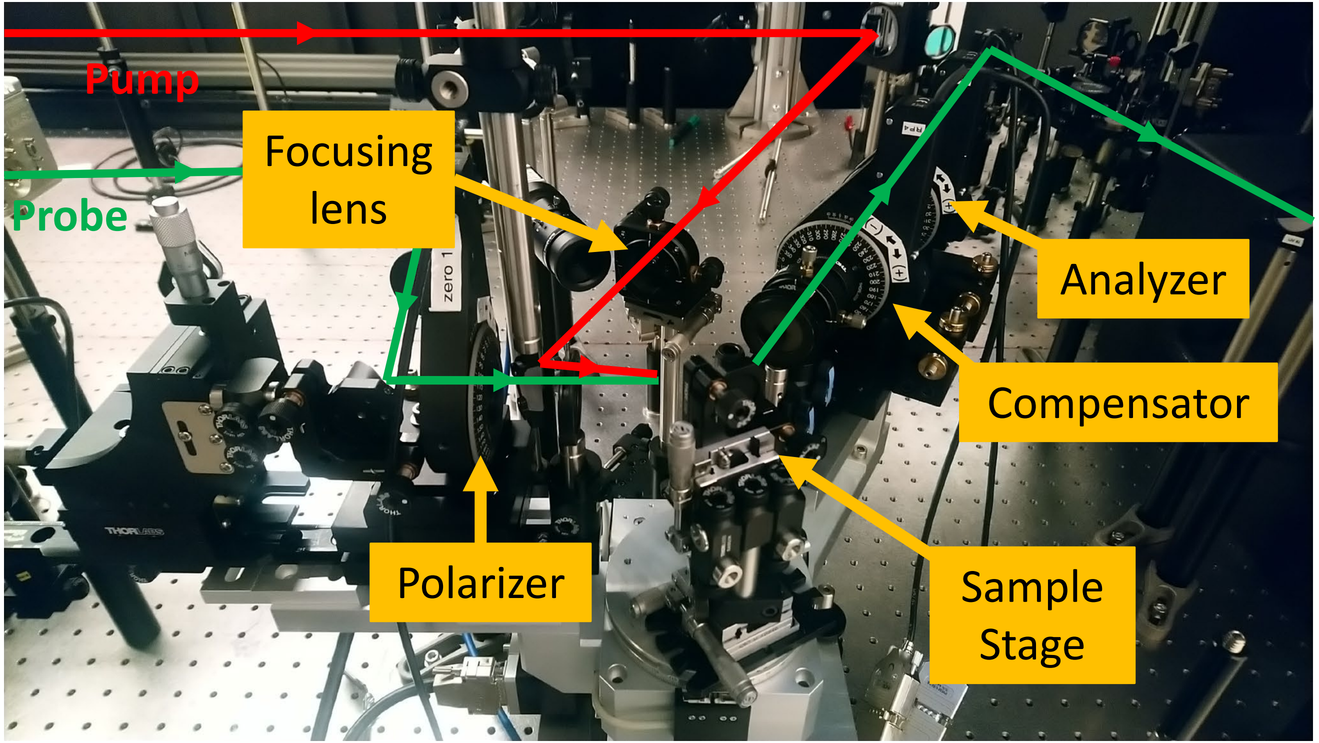

Rotating compensator ellipsometer:

Compensator was rotated in steps of 10º for a total of 55-65 angles.

Probe beam of 350-750 nm at 60º incidence angle.

P-polarized pump beam: 35 fs pulses of 800 nm wavelength at 1 kHz repetition rate.

Delay time from -10 to 50 ps.

Time resolution of about 500 fs.

Espinoza et al., APL **115**, 052105 (2019).

Pseudo-dielectric constant as function of delay time

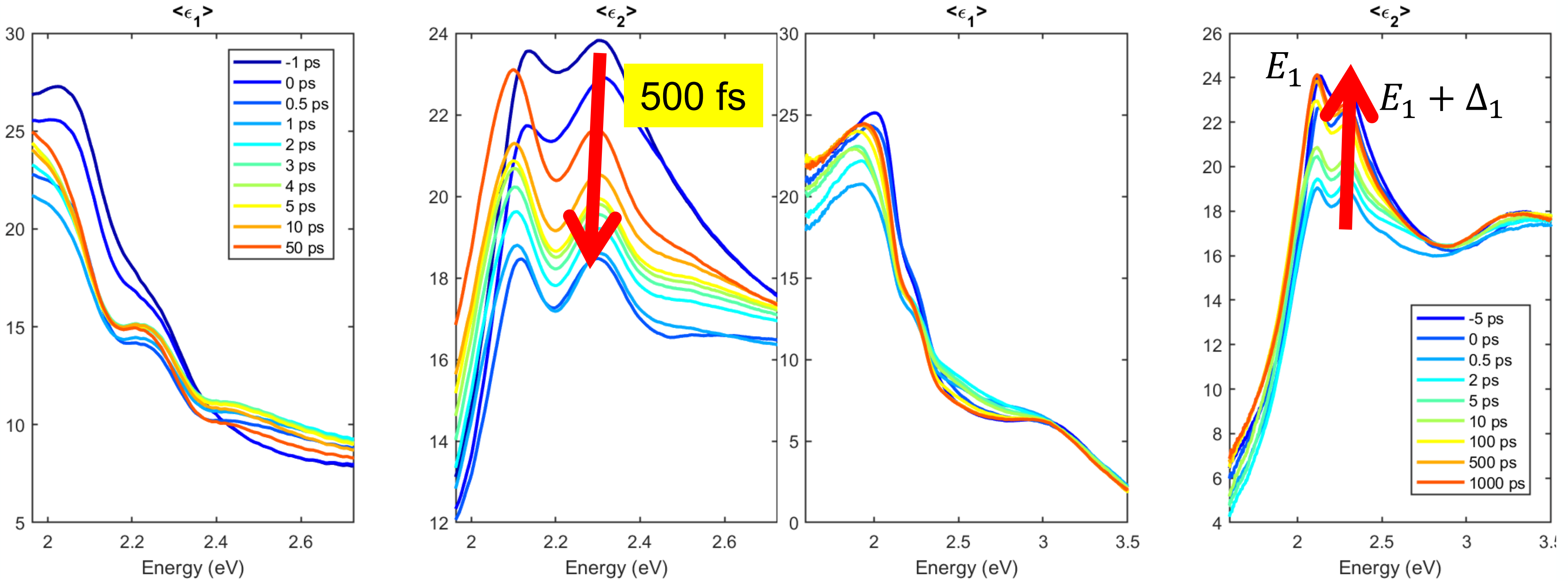

Rapid decrease of ε within first 500 fs.

Recovery takes 1 ns or longer.

Carlos A. Armenta, Shirly J. Espinoza (unpublished)

2D excitons with band filling - no screening

$$\varepsilon_2(E) = \frac{e^2 \mu_\perp^{(E_1)} \bar{P}^2}{6\varepsilon_0 m^2 \pi} \mathrm{Im}\left\{\frac{\{g_a[\xi(E+i\Gamma)] + g_a[\xi(-E-i\Gamma)] - 2g_a[\xi(0)]\}}{(E+i\Gamma)^2}\right\} \int_{-k_{\max}}^{k_{\max}} \{1 - f[E_c(E, k_z^2)]\} dk_z$$

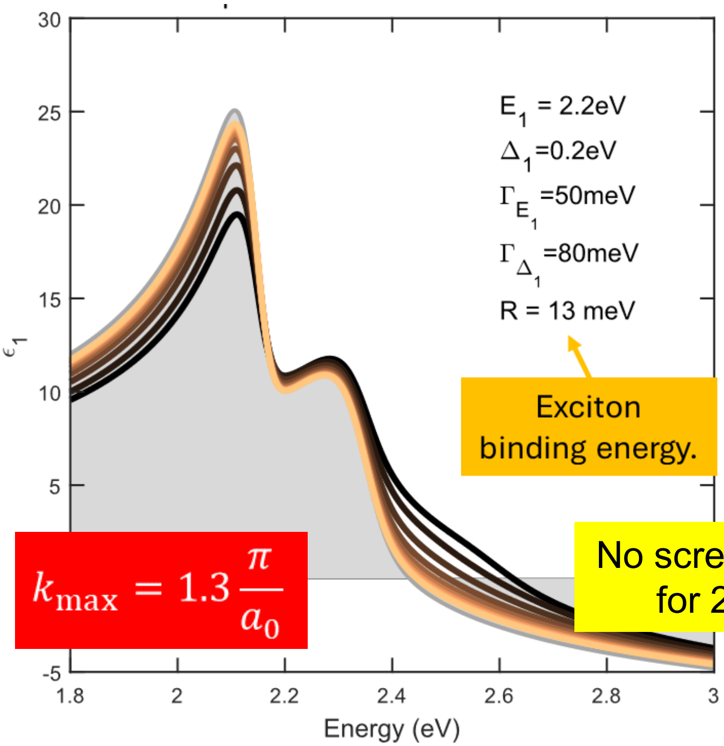

$$k_{\max} = 1.3\frac{\pi}{a_0}$$

No screening included for 2D excitons

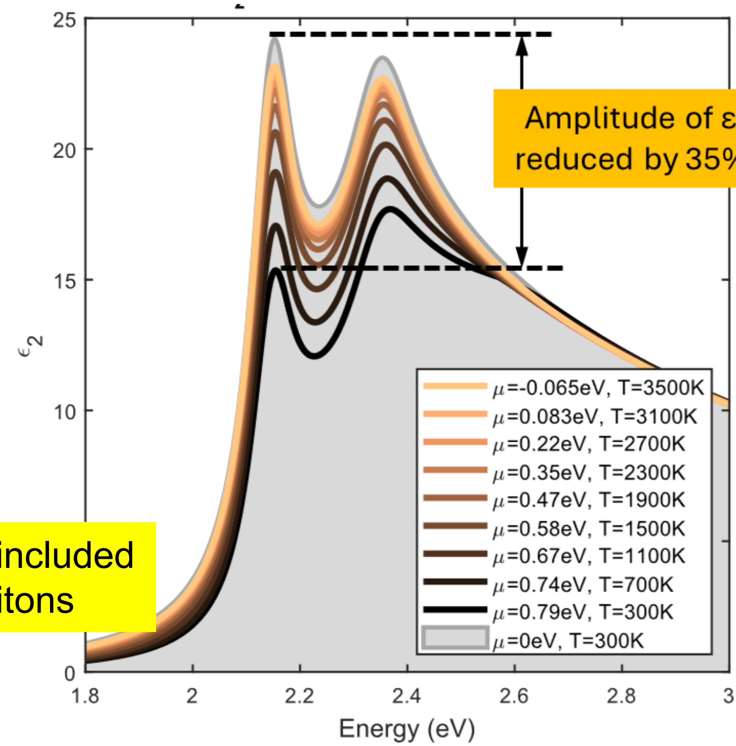

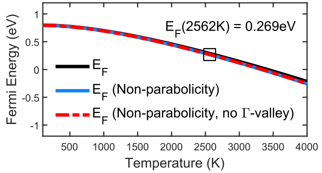

Band-filling effects

We combine Tanguy's line shape for 2D excitons with Xu's band-filling model:

$$\varepsilon_2(E) = \frac{e^2\mu_\perp^{(E_g)}\bar{P}^2}{6\varepsilon_0 m^2\pi}\,\mathrm{Im}\left\{\frac{\{g_a[\xi(E+i\Gamma)] + g_a[\xi(-E-i\Gamma)] - 2g_a[\xi(0)]\}}{(E+i\Gamma)^2}\right\}\int_{-k_{\max}}^{k_{\max}}\{1 - f[E_c(E,k_z^2)]\}dk_z$$

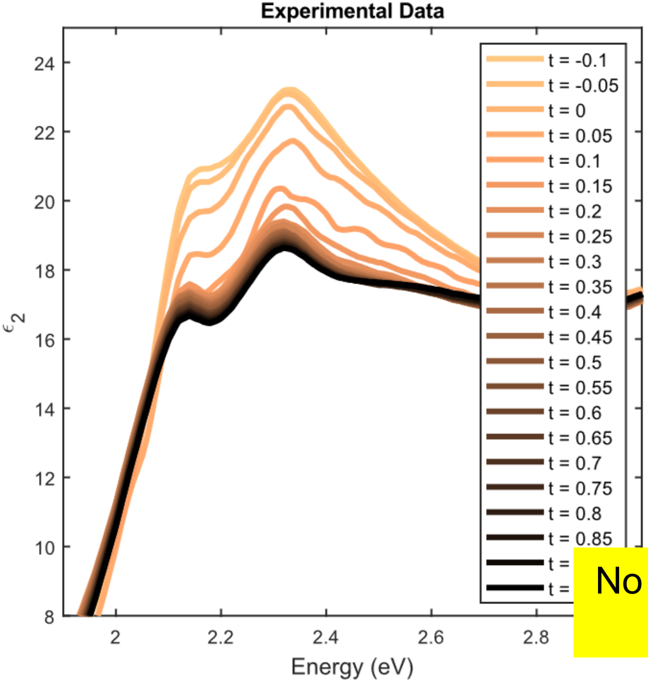

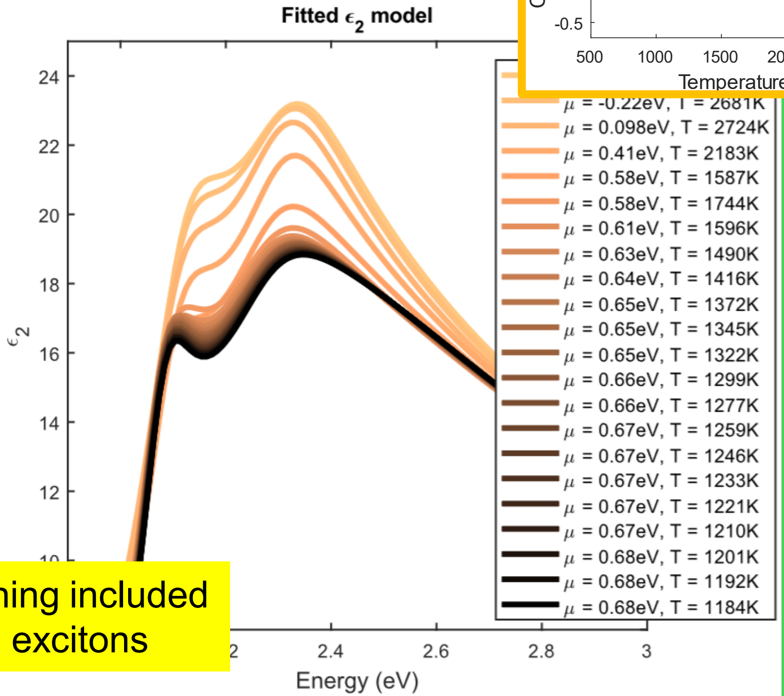

No screening included for 2D excitons

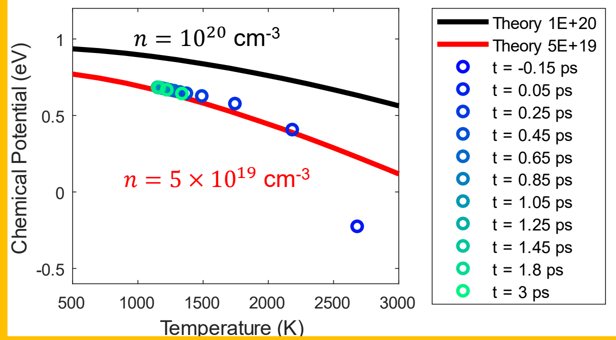

Simulation of the chemical potential as a function of temperature for different carrier densities.

Carlos A. Armenta, Shirly J. Espinoza (unpublished)

C. Xu, J. Appl. Phys. **125**, 085704 (2019).
C. Xu, Phys. Rev. Lett. **118**, 267402 (2017).

Summary: Screening of excitons

- Excitonic direct gap absorption: **3D hydrogen problem with Coulomb potential** treated in every quantum mechanics course
  Sommerfeld enhancement of the absorption.
- Screened exciton absorption: 3D hydrogen problem with **Yukawa potential**
  Not solvable analytically, use Hulthen potential (Banyai & Koch, Haug & Koch)
  Sommerfeld enhancement persists well above the Mott transition.
- Excitonic direct gap absorption in 2D materials or E_1 excitons
  2D hydrogen problem with Coulomb potential (Flügge: Rechenmethoden der QM)
- **Excitonic 2D-transitions at E_1 with screening (femtosecond ellipsometry)**
  No known solution for screened Sommerfeld enhancement in 2D.

Conclusions

- Quantitative modeling of low-density optical processes is possible with basic physics and matrix elements from k.p theory:
  - Photoluminescence in Ge (Menendez)
  - Indirect gap absorption in Ge (Menendez)
  - **Direct gap absorption in Ge at low T (excitons in 3D); E_1 critical points in Ge (excitons in 2D)**
  - More work is needed at high temperatures and for materials other than Ge.
- High carrier excitations:
  - High electron doping density in Ge
  - **Thermal excitation of electron-hole pairs in InSb and α-tin (3D screening and band filling).**
  - **Femtosecond laser generation of electron-hole pairs in Ge (2D screening)**
  - Experimental data and qualitative explanations exist
- We need more experiments and more detailed theory and simulations.

Thank you!

Questions?

Many students contributed to this project.

http://femto.nmsu.edu

Biography

Regensburg/Stuttgart
Germany

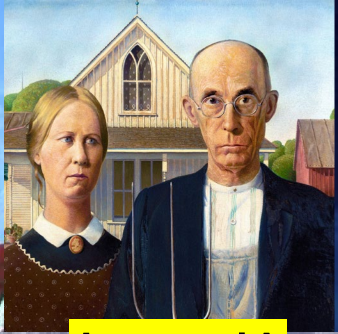

Ames, IA

Motorola (Mesa, Tempe)
Arizona, 1997-2005

Freescale, IBM
New York, 91-92; 07-10

NMSU
Las Cruces, NM
Since 2010

Motorola, Freescale
Texas, 2005-2007

Where is Las Cruces, NM ???

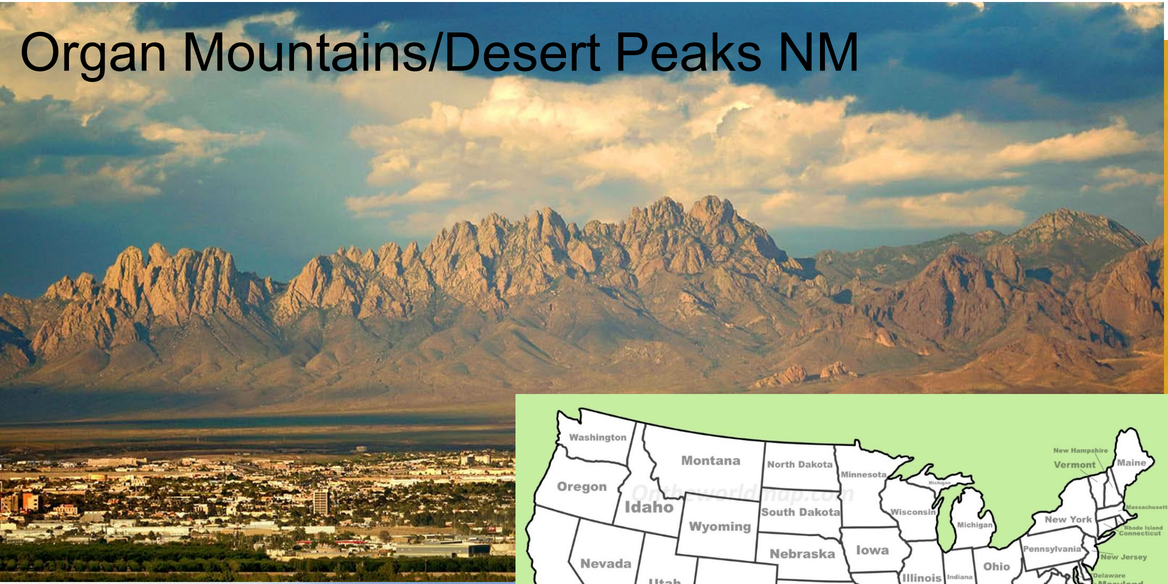
Organ Mountains/Desert Peaks NM

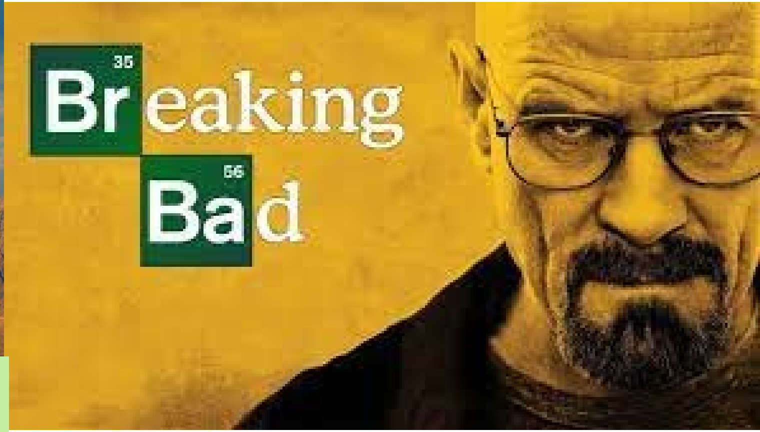

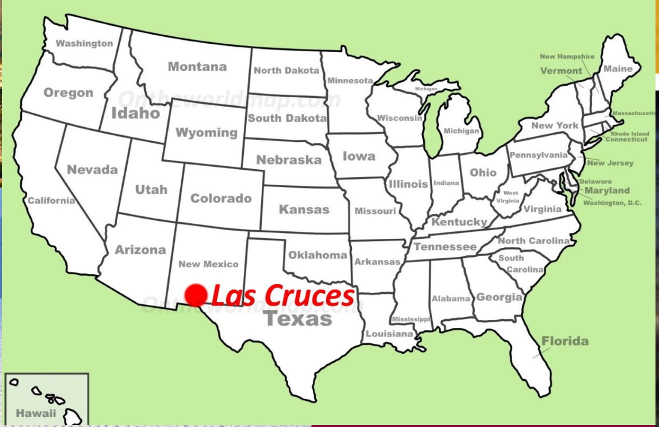


White Sands NP

Ge Band structure: where did this come from?

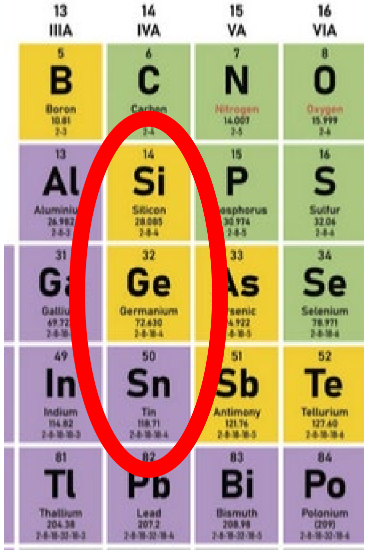

Darwin shift

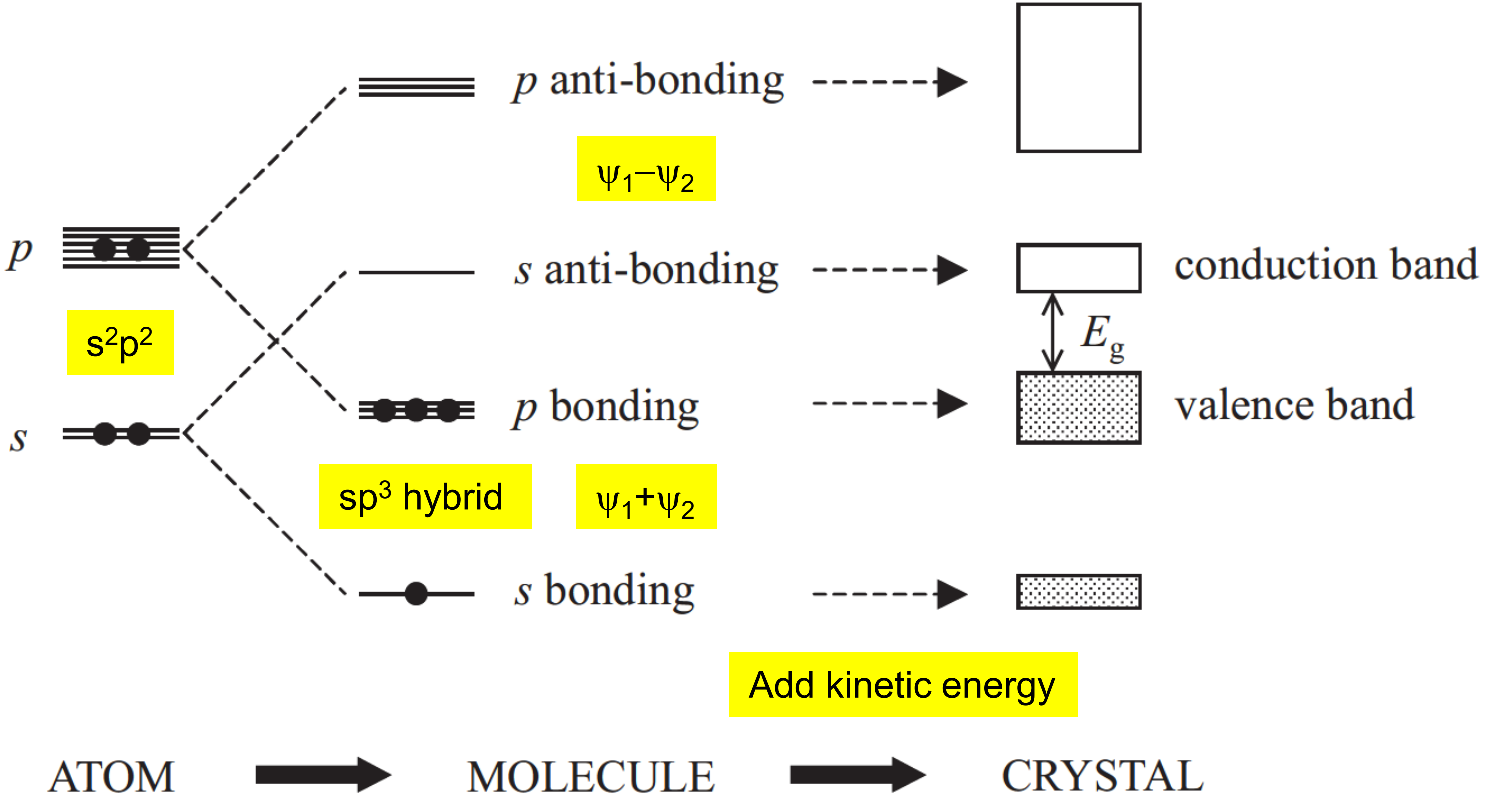

$\psi_1 - \psi_2$

s^2p^2

sp^3 hybrid

$\psi_1 + \psi_2$

Add kinetic energy

Works well for Ge, GaAs, etc.

Fox, Chapter 3

Critical points in the dielectric function of Ge

- Peaks in the dielectric function
- Due to interband transitions from valence to conduction band (electron-hole pairs)

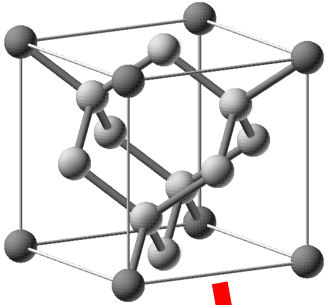

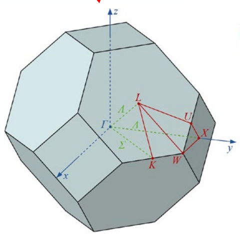

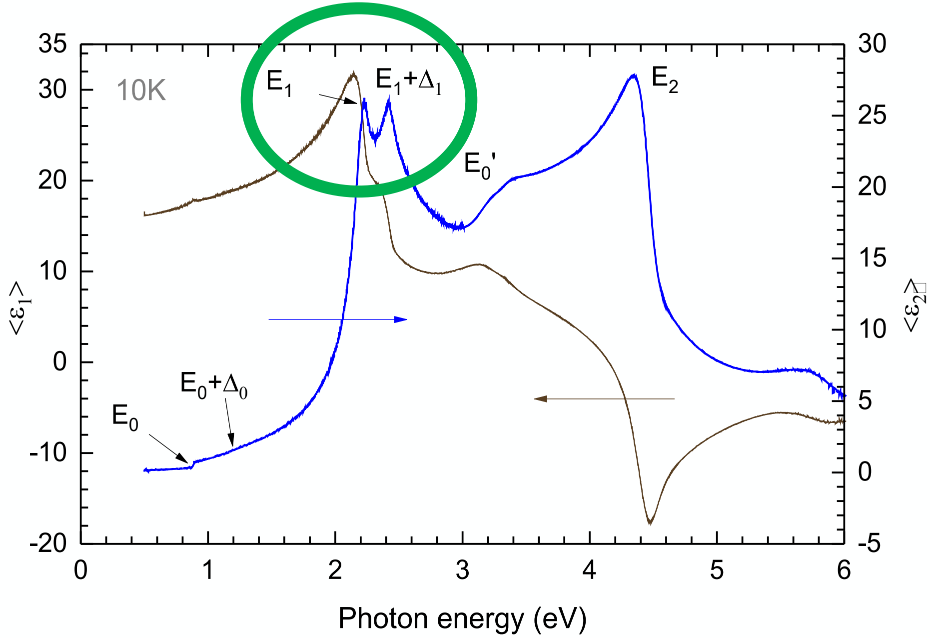

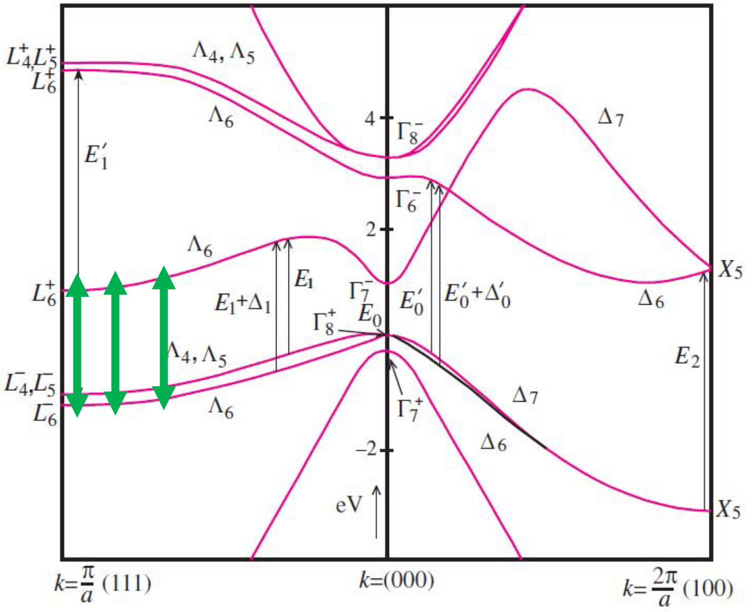

$$\psi(\vec{r}) = e^{i\vec{k}\cdot\vec{r}}u_{n,\vec{k}}(\vec{r})$$

P.Y. Yu and M. Cardona, *Fundamentals of Semiconductors*.

Two-dimensional Bohr problem

$$H=-\frac{\hbar^2}{2\mu_\perp}\left(\frac{\partial^2}{\partial x^2}+\frac{\partial^2}{\partial y^2}\right)-\frac{\hbar^2}{2\mu_\parallel}\frac{\partial^2}{\partial z^2}-\frac{e^2}{\varepsilon_r r}$$

Assume that $\mu_{||}$ is infinite (separate term).
Use cylindrical coordinates.
Separate radial and polar variables.
Similar Laguerre solution as 3D Bohr problem.

$$a_X=\frac{4\pi\varepsilon_0\varepsilon_r\hbar^2 m_0}{\mu_\perp\mu e^2}$$

$$R=\frac{\mu_\perp e^4}{2\hbar^2 m_0(4\pi\varepsilon_0\varepsilon_r)^2}$$

$$E_n=-\frac{R}{\left(n-\frac{1}{2}\right)^2},\qquad n=1,2,\ldots$$

Half-integral quantum numbers

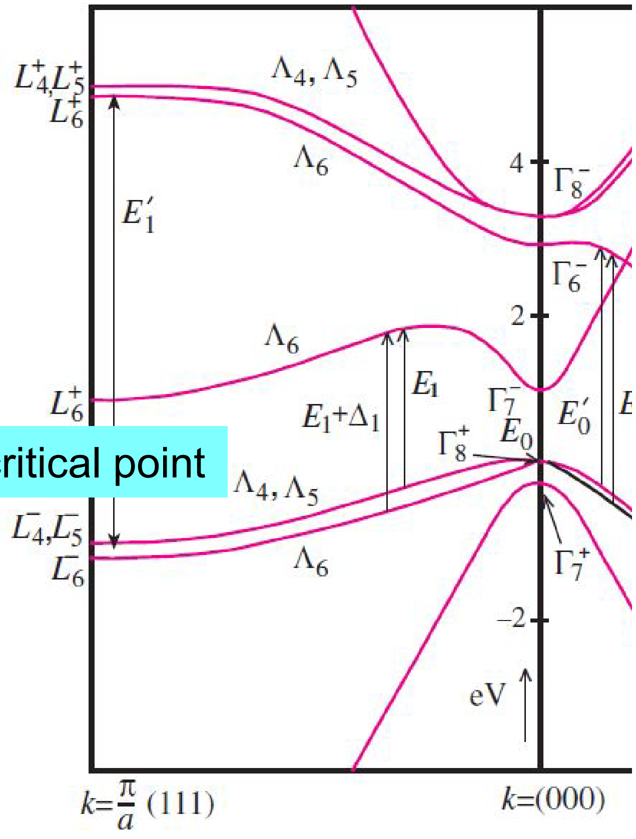

2D critical point

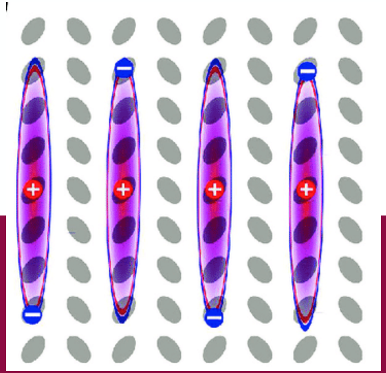

M. Shinada and S. Sugano, J. Phys. Soc. Jpn. **21**, 1936 (1966).

Two-dimensional saddle-point excitons (E_1, $E_1+\Delta_1$)

$$\varepsilon(E) = \frac{A}{(E+i\Gamma)^2}\{g[\xi(E+i\Gamma)] + g[\xi(-E-i\Gamma)] - 2g[\xi(0)]\}$$

$$g(\xi) = 2\ln(\xi) - 2\psi(\frac{1}{2} - \xi)$$

$$\psi(z) = \frac{d\ln\Gamma(z)}{dz}$$

$$\xi(z) = \sqrt{R/_{E_0 - z}}$$

$$A = \frac{\mu e^2}{3\pi\varepsilon_0 m_0^2}|P|^2$$

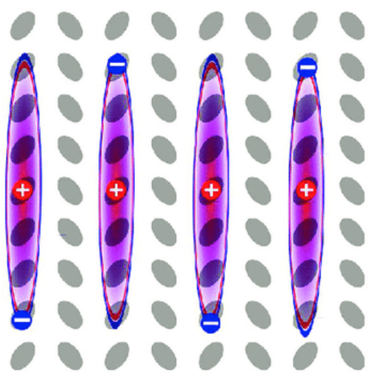

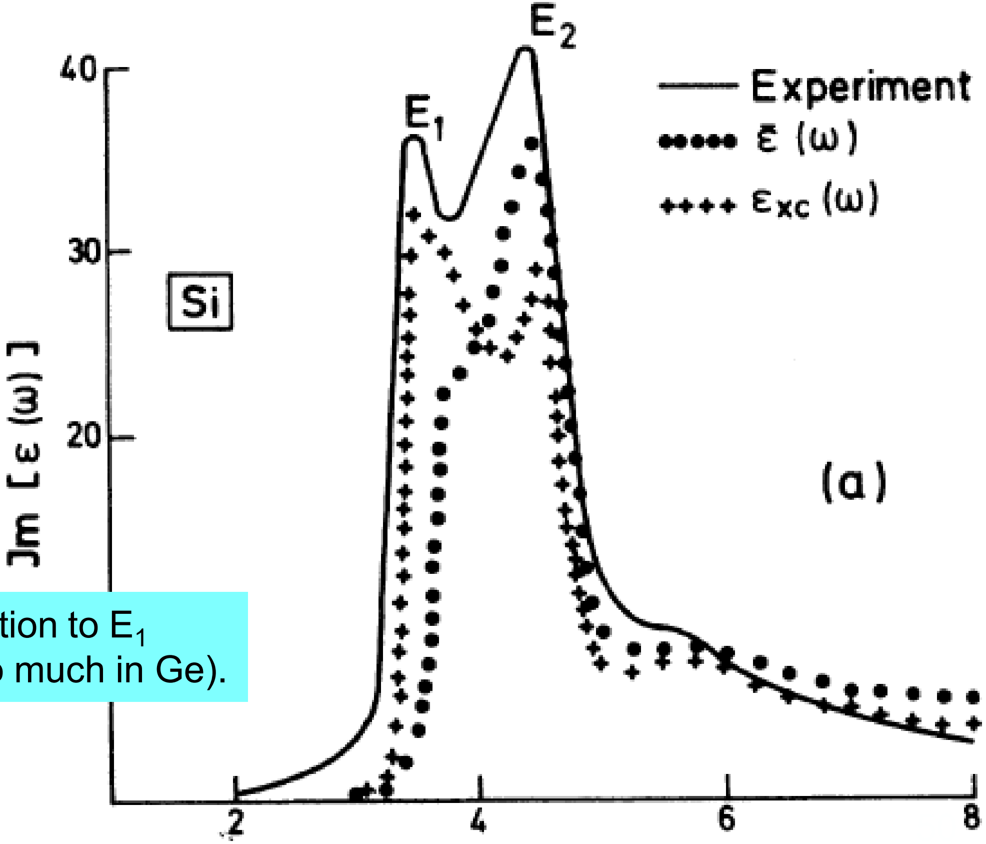

Strong excitonic contribution to E_1 critical point in Si (mot so much in Ge).

B. Velicky and J. Sak, phys. status solidi **16**, 147 (1966)
C. Tanguy, Solid State Commun. **98**, 65 (1996)
W. Hanke and L.J. Sham, Phys. Rev. B **21**, 4656 (1980)

Comparison with experimental data

$$\varepsilon(E, E_1, \Gamma, R, k_{\max}) = \frac{k_{\max} e^2 \bar{P}^2 \mu_\perp^{(E_1)}}{3\varepsilon_0 m^2 \pi (E + i\Gamma)^2} \left\{ g_a \left[\sqrt{\frac{R}{E_1 - (E + i\Gamma)}} \right] + g_a \left[\sqrt{\frac{R}{E_1 - (-E - i\Gamma)}} \right] - 2 g_a \left[\sqrt{\frac{R}{E_1 - (0)}} \right] \right\}$$

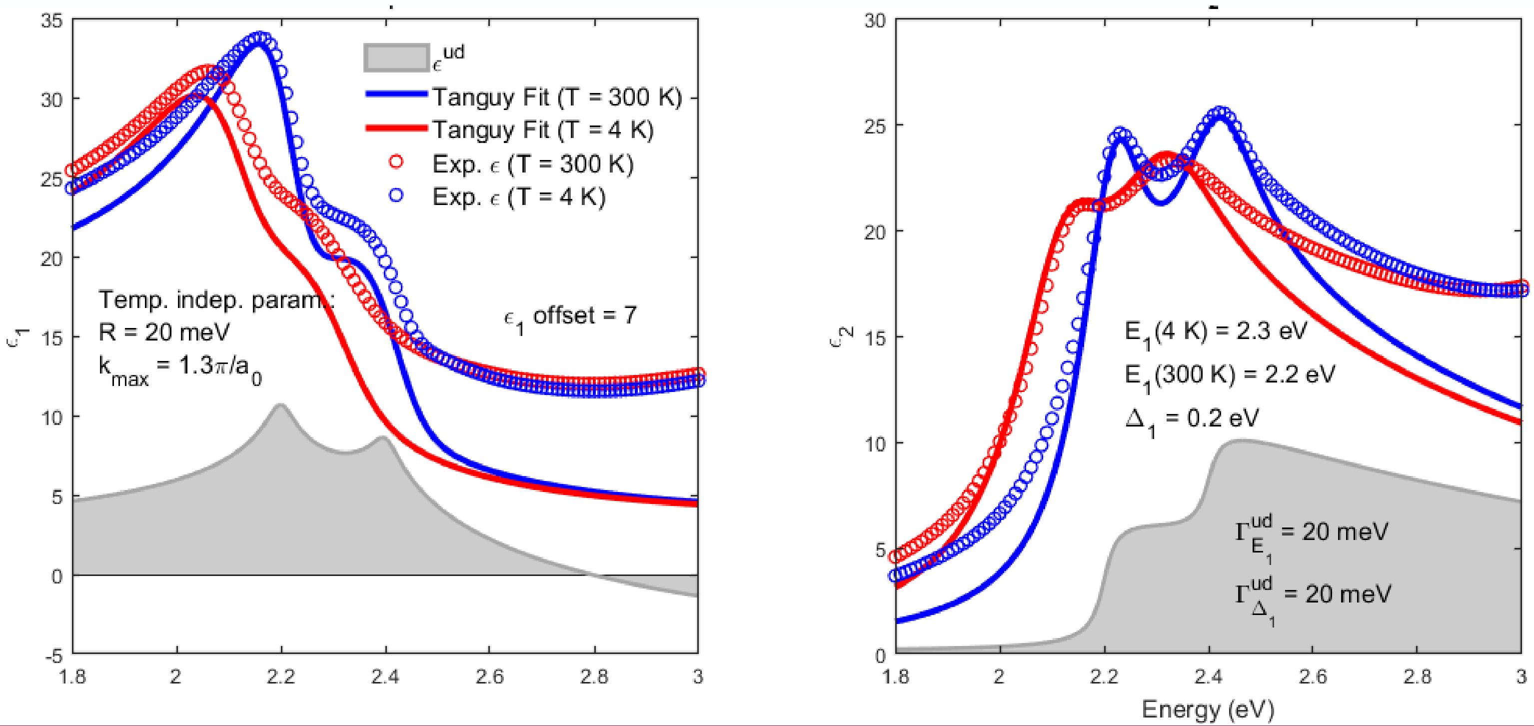

Experimental data:

Emminger (5 K), JVST B **38**, 012202 (2020).

Nunley (300 K), JVST B **34**, 061205 (2016)

Optical Absorption at High Carrier Densities

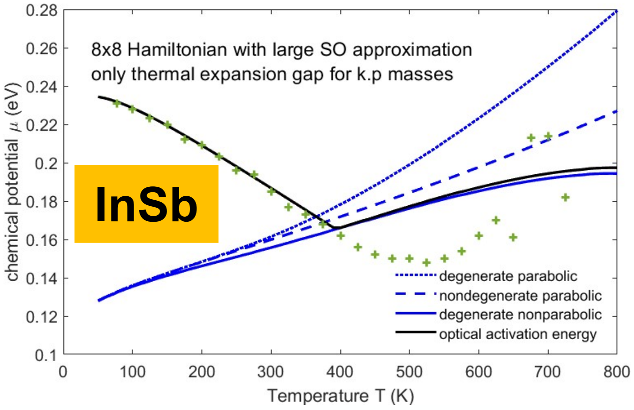

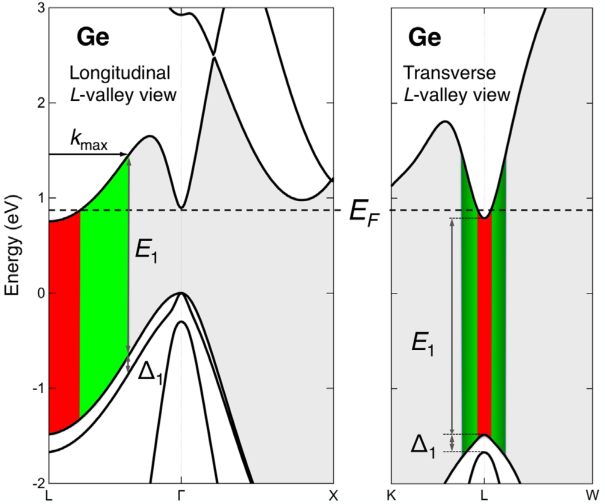

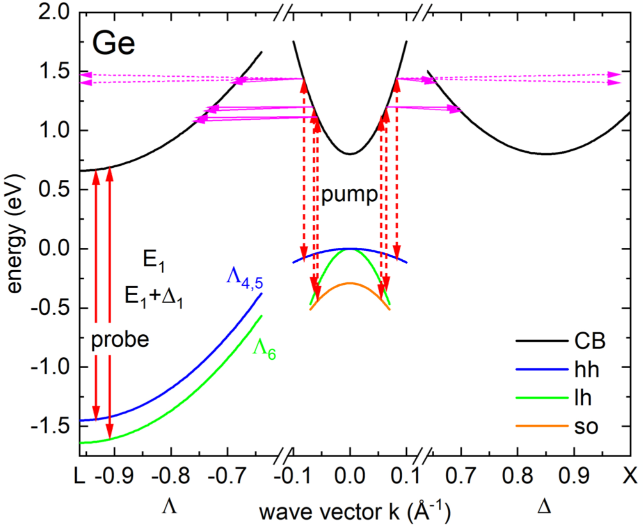

High temperature
(thermal excitation of e-h pairs)
constant m and E_0

High n-doping of Ge with P
(free electrons pile up at L-point)

Intense femtosecond **laser excitation** (ELI Beamlines)
(electrons pile at L-point)

Rivero, JVSTB **41**, 022203 (2023) Xu et al., PRL **118**, 267402 (2017) Espinoza, APL **115**, 052105 (2019)